



SAPIENZA
UNIVERSITÀ DI ROMA



Dipartimento di Chimica e Tecnologie del Farmaco
Ph.D. in Pharmaceutical Sciences
(XXIII cycle 2007 – 2010)

Rational Design of Novel Antiviral Compounds Through Computational Approaches

Mentor:
Prof. Rino Ragno

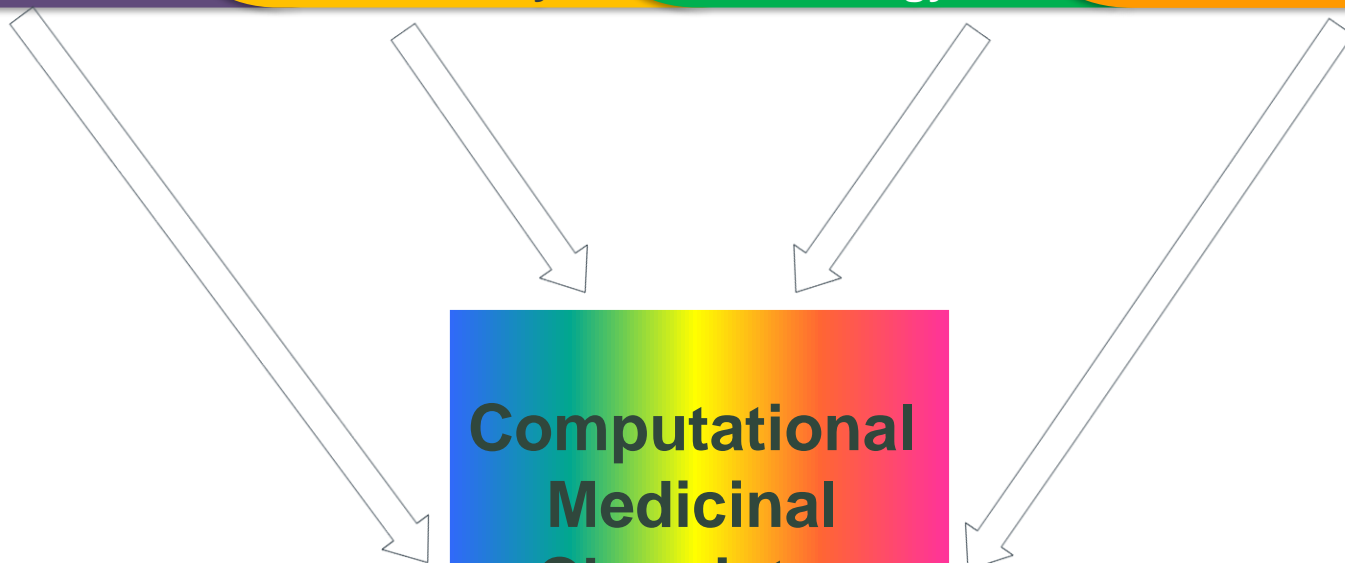
Candidate:
Ira Musmuça

Chemoinformatics

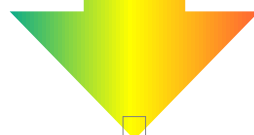
Computational
Chemistry

Computational
Biology

Bioinformatics



Computational
Medicinal
Chemistry



Drug

Advantages

1. **Orders of Magnitude Cheaper and Faster**
2. Offers the Possibility to Predict Molecular Behaviours that Cannot be Elucidated in any Other Way
3. Simulation of Complex Molecular Environments, Widening the Applicability of *in silico* Studies from the Interactions of Small Molecules with Key Protein Residues, to the Simulation of the Dynamic Evolution of Complex Biological Systems with Atomic Resolution

Advantages

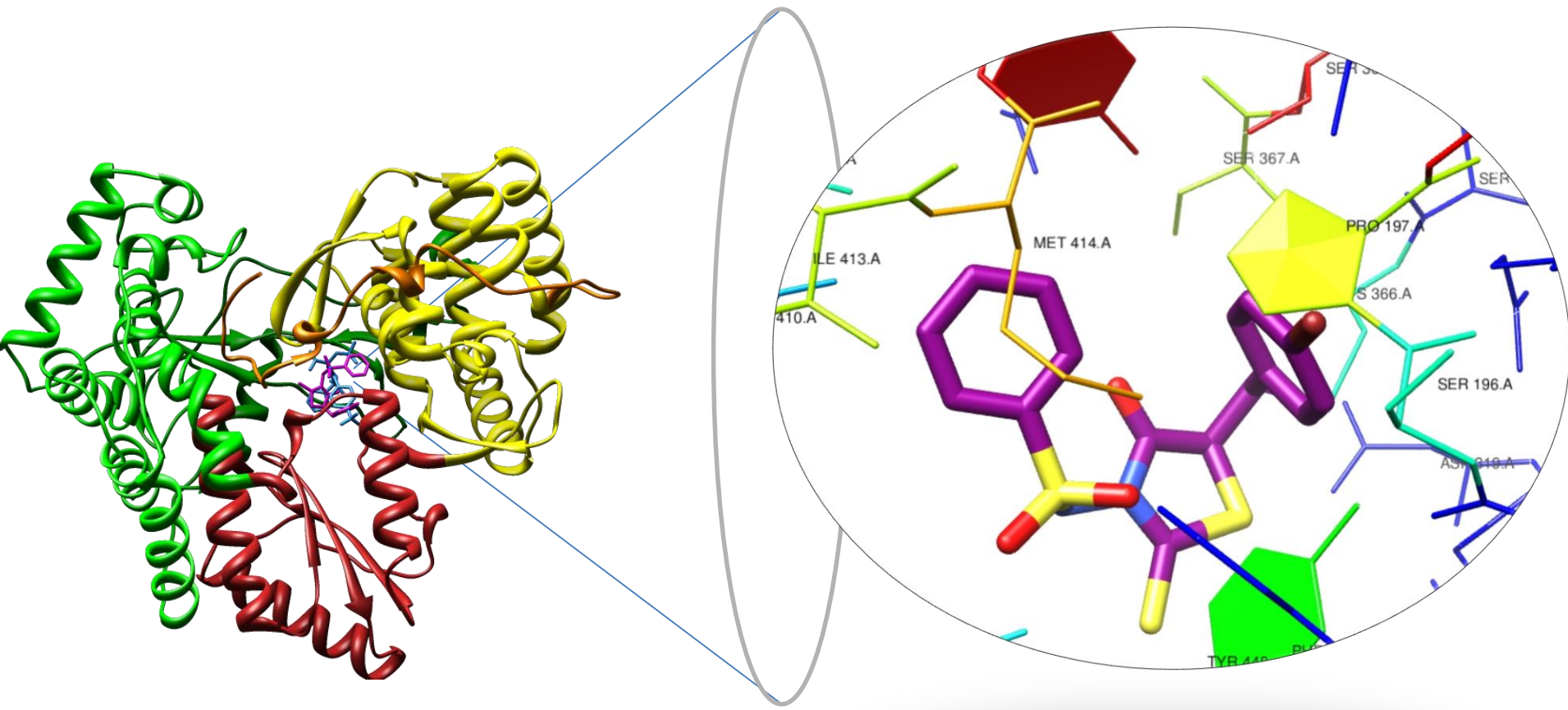
1. Orders of Magnitude Cheaper and Faster
2. **Offers the Possibility to Predict Molecular Behaviours that Cannot be Elucidated in any Other Way**
3. Simulation of Complex Molecular Environments, Widening the Applicability of *in silico* Studies from the Interactions of Small Molecules with Key Protein Residues, to the Simulation of the Dynamic Evolution of Complex Biological Systems with Atomic Resolution

Advantages

1. Orders of Magnitude Cheaper and Faster
2. Offers the Possibility to Predict Molecular Behaviours that Cannot be Elucidated in any Other Way
3. **Simulation of Complex Molecular Environments, Widening the Applicability of *in silico* Studies from the Interactions of Small Molecules with Key Protein Residues, to the Simulation of the Dynamic Evolution of Complex Biological Systems with Atomic Resolution**

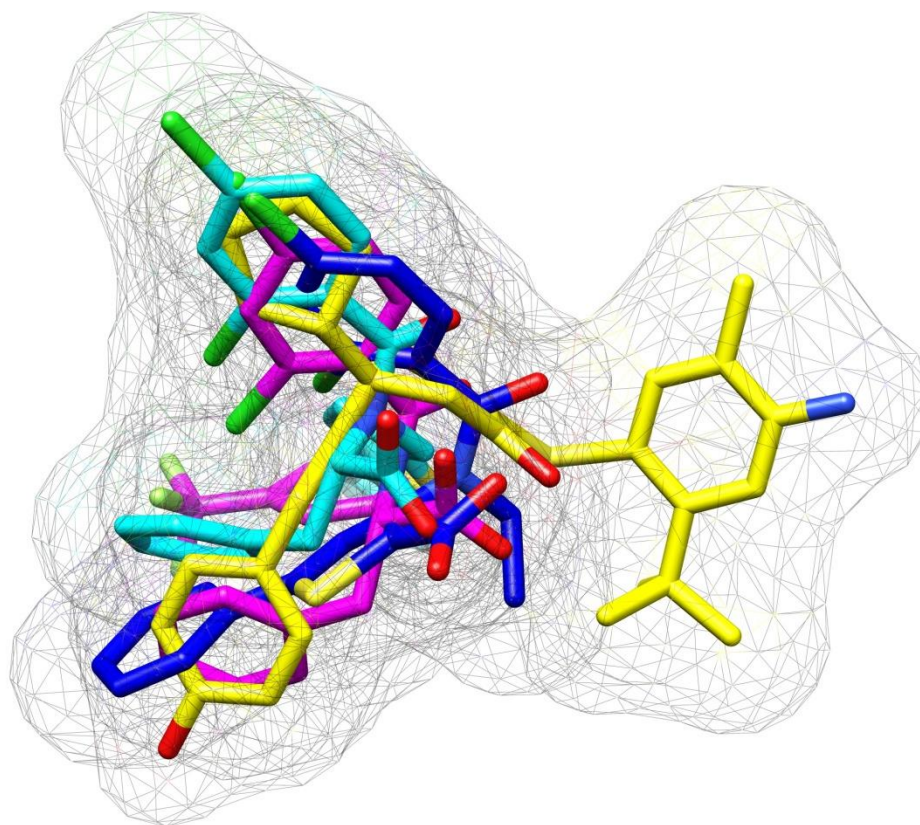
Broad Classification

- 1. Structure – Based Approaches
- 2. Ligand – Based Approaches



Broad Classification

1. Structure – Based Approaches
- 2. Ligand – Based Approaches**



Development and Application of Medicinal Chemistry Computational Methods in the Research Area of QSAR, 3D-QSAR, Molecular Docking and Virtual Screening

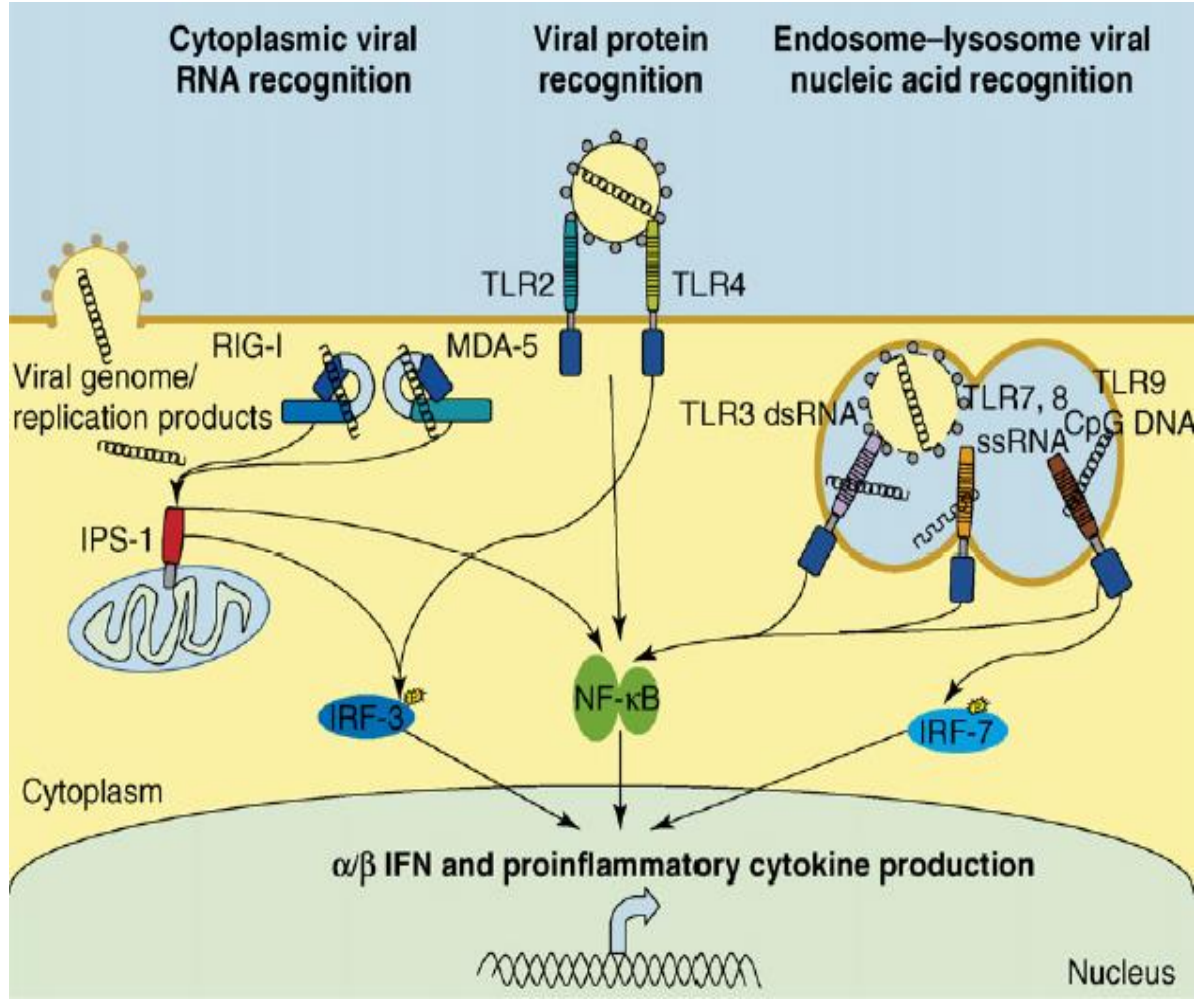
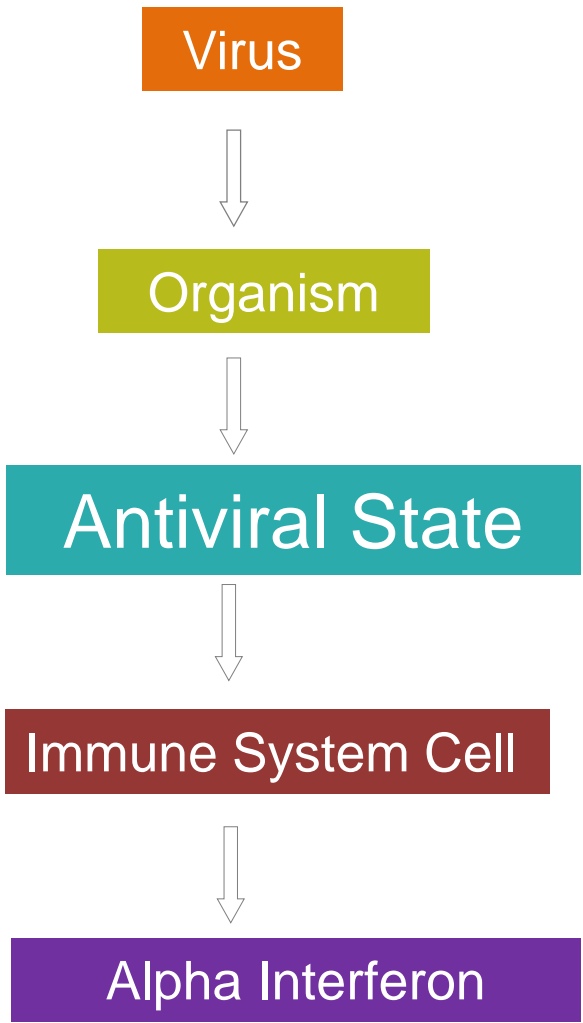
- Orally Active Interferon Inducers
- Allosteric Inhibitors of HCV NS5B RNA-dependent RNA Polymerase

Small-Weight Interferon Inducers Orally Active vs Hepatitis C Virus

Aim of the Work

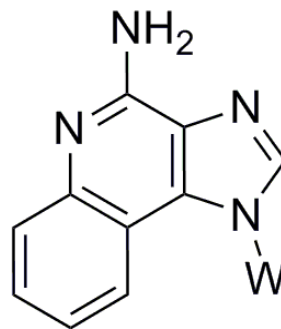
Description of How Steric, Electrostatic, Hydrophobic and Hydrogen-Bonding Interactions Might Influence the Biological Activity of a Published Set of 176 IFN Inducers, Using a Ligand-Based 3D-QSAR Approach

Interferon Inducers



Current Opinion in Immunology 2007, 19, 17-23

- ❖ Polynucleotides
- ❖ Fluorenones
- ❖ Pyrimidinones
- ❖ Anthraquinones

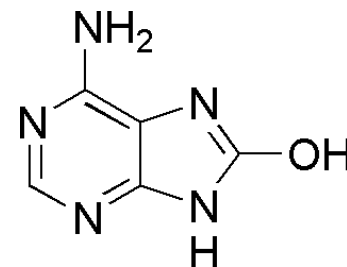
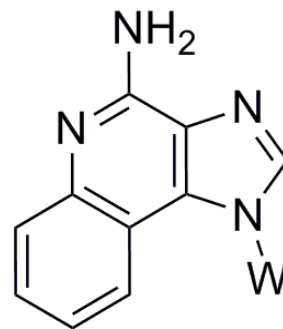


- ❖ 1H-imidazo-[4,5-c]quinolines

**Small Weight Molecules with
in vitro and *in vivo* alpha-IFN
Inducing Activity**



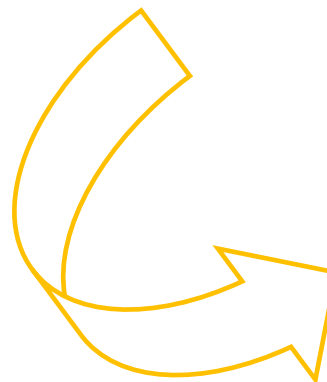
- ❖ Polynucleotides
- ❖ Fluorenones
- ❖ Pyrimidinones
- ❖ Anthraquinones



Small Weight Molecules with *in vitro* and *in vivo* alpha-IFN Inducing Activity

- ❖ 1H-imidazo-[4,5-c]quinolines
- ❖ 8-hydroxyadenines

Hirota et al. *J. Med. Chem.* **2002**, *45*, 5419-5422
Isobe et al. *J. Med. Chem.* **2006**, *49*, 2088-2095.
Isobe et al. *Bioorg. Med. Chem.* **2003**, *11*, 3641-3647
Kurimoto et al. *Bioorg. Med. Chem.* **2003**, *11*, 5501-5508
Kurimoto et al. *Bioorg. Med. Chem.* **2004**, *12*, 1091-1099
Gerster et al. *J. Med. Chem.* **2005**, *48*, 3481-3491



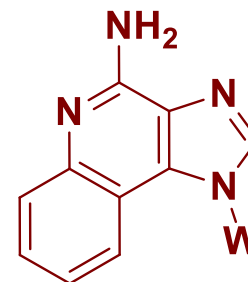
- Relationships Between Chemical-Physical Properties of Chemical Substances and their Biological Activities to Obtain a Reliable Statistical Model for Prediction of the Activities of New Chemical Entities

Primary Aims of QSAR

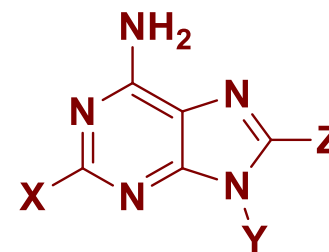
- Optimization of the Existing Leads so to Improve Their Biological Activities.
- Prediction of the Biological Activity of Untested and Sometimes yet Unavailable Compounds

QSAR → 3D-QSAR

- **Training Set Selection**
- Molecular Modeling
- Molecular Alignment
- Molecular Interaction Fields
- Statistical Analysis
- External Validation
- GRID Plot Interpretation



1H-imidazo[4,5-c]quinolines⁶



Adenines Derivatives¹⁻⁵

¹ Hirota et al. *J. Med. Chem.* **2002**, *45*, 5419-5422

² Isobe et al. *J. Med. Chem.* **2006**, *49*, 2088-2095.

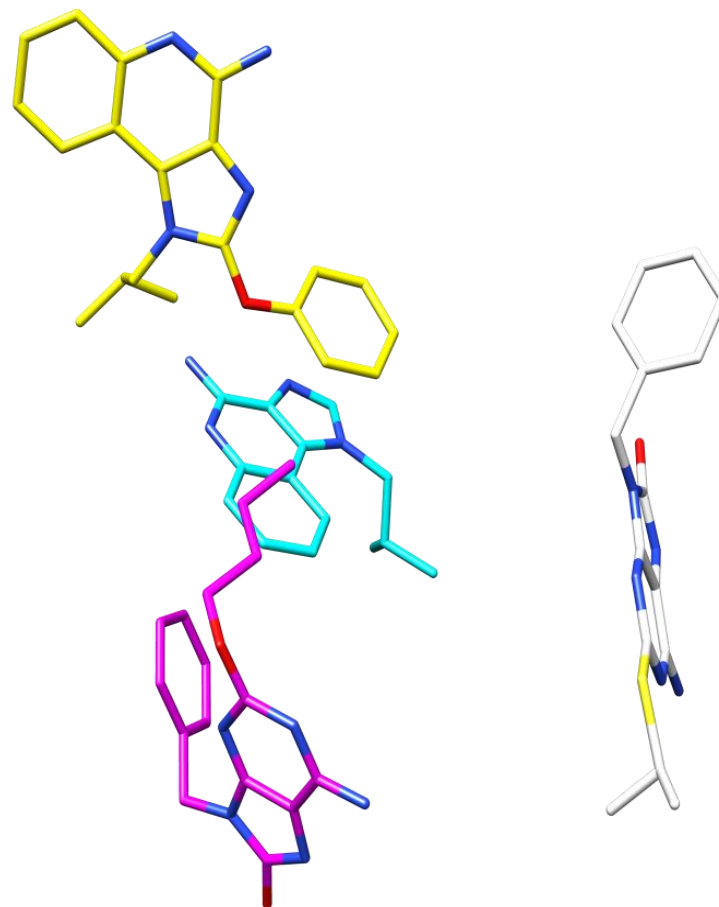
³ Isobe et al. *Bioorg. Med. Chem.* **2003**, *11*, 3641-3647

⁴ Kurimoto et al. *Bioorg. Med. Chem.* **2003**, *11*, 5501-5508

⁵ Kurimoto et al. *Bioorg. Med. Chem.* **2004**, *12*, 1091-1099

⁶ Gerster et al. *J. Med. Chem.* **2005**, *48*, 3481-3491

- Training Set Selection
- **Molecular Modeling**
- Molecular Alignment
- Molecular Interaction Fields
- Statistical Analysis
- External Validation
- GRID Plot Interpretation

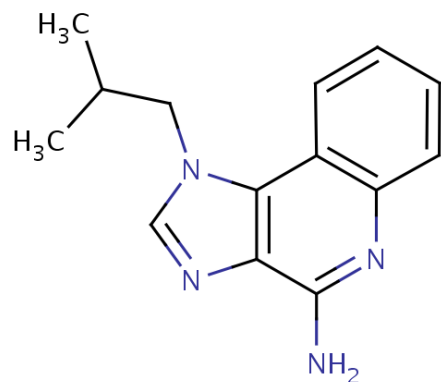


¹ Schuttelkopf et al. PRODRG: a tool for high-throughput crystallography of protein-ligand complexes. *Acta Crystallogr. D Biol. Crystallogr.* **2004**, *60*, 1355-1363

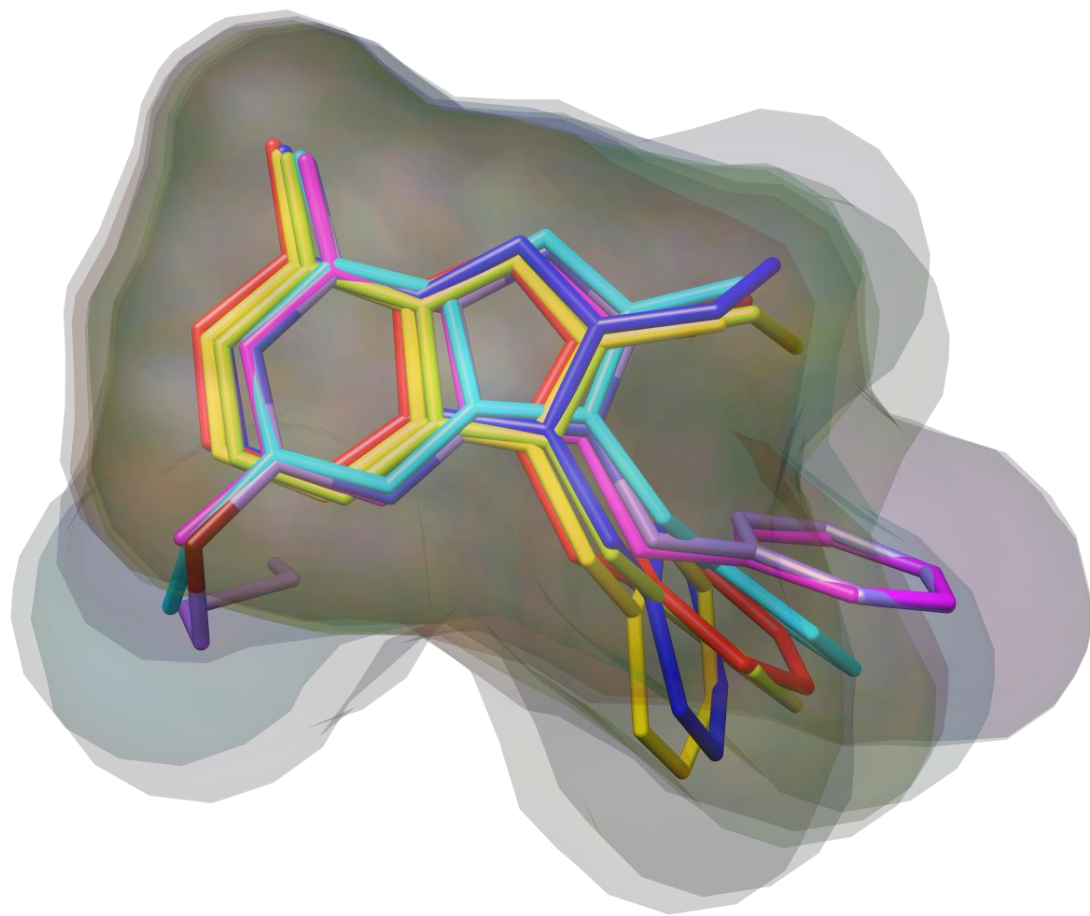
² Van Aalten et al. *J. Comput. Aided Mol. Des.* **1996**, *10*, 255-262

³ Berendsen et al. GROMACS: A message-passing parallel molecular dynamics implementation. *Comput. Phys. Commun.* **1995**, *91*, 43-56

- Training Set Selection
- Molecular Modeling
- **Molecular Alignment**
- Molecular Interaction Fields
- Statistical Analysis
- External Validation
- GRID Plot Interpretation

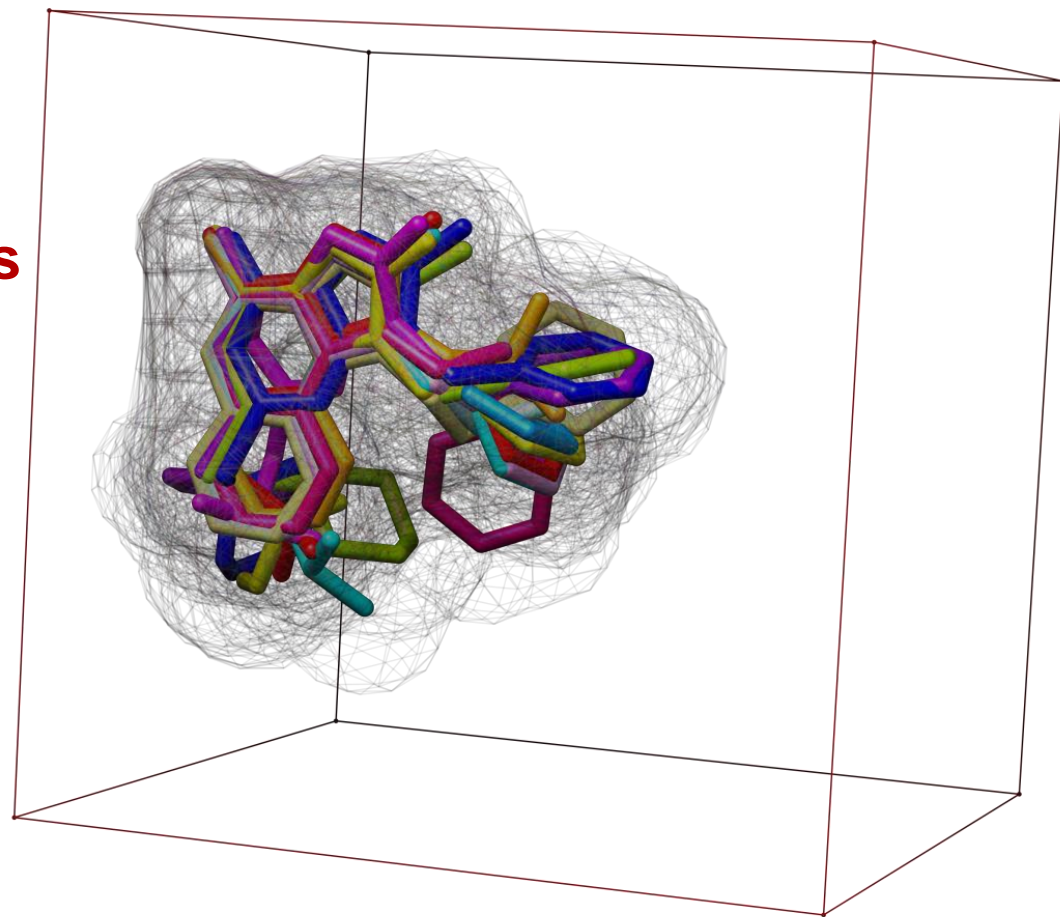


Imiquimod



¹ Jain, A. N. Ligand-based structural hypotheses for virtual screening. *J. Med. Chem.* **2004**, *47*, 947-961

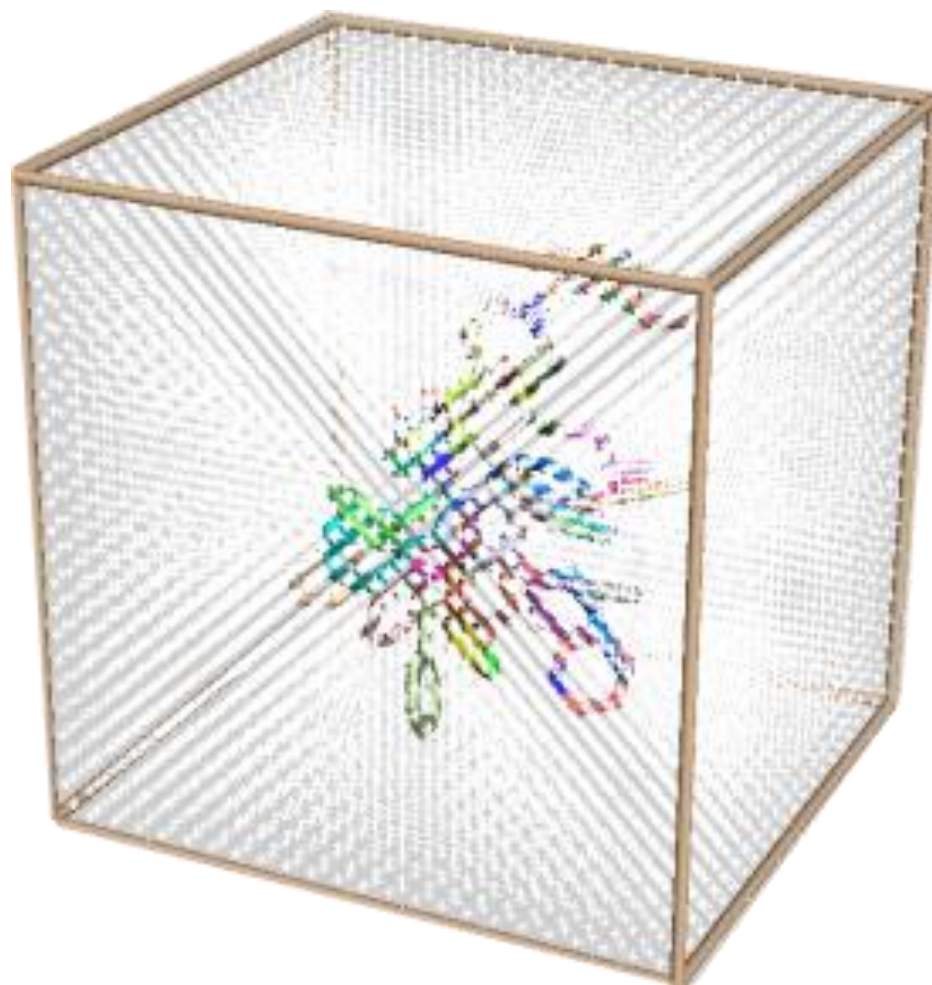
- Training Set Selection
- Molecular Modeling
- Molecular Alignment
- **Molecular Interaction Fields**
- Statistical Analysis
- External Validation
- GRID Plot Interpretation



Wade, R. C. Molecular Interaction Fields, In: *3D QSAR in Drug Design. Theory, Methods and Applications*, Kubinyi, H. Ed.; ESCOM, Leiden, Netherlands, 1993, pp. 486-505.

Goodford, P. J. A computational procedure for determining energetically favorable binding sites on biologically important macromolecules. *J. Med. Chem.* **1985**, 28, 849-857.

- Training Set Selection
- Molecular Modeling
- Molecular Alignment
- **Molecular Interaction Fields**
- Statistical Analysis
- External Validation
- GRID Plot Interpretation



Wade, R. C. Molecular Interaction Fields, In: *3D QSAR in Drug Design. Theory, Methods and Applications*, Kubinyi, H. Ed.; ESCOM, Leiden, Netherlands, 1993, pp. 486-505.

Goodford, P. J. A computational procedure for determining energetically favorable binding sites on biologically important macromolecules. *J. Med. Chem.* **1985**, *28*, 849-857.

- Training Set Selection
- Molecular Modeling
- Molecular Alignment
- Molecular Interaction Fields
- **Statistical Analysis**
- External Validation
- GRID Plot Interpretation

Squared Correlation Coefficient

$$r^2 = 1 - \frac{\sum_{i=1}^N (Y_{\text{exp},i} - Y_{\text{calc},i})^2}{\sum_{i=1}^N (Y_{\text{exp},i} - \bar{Y})^2}$$

$$0 \leq r^2 \leq 1$$

r^2 measures of the 'simultaneous' variable variation

$r^2 = 0$: the statistical model is not able to explain data

$r^2 = 1$: the statistical model is perfectly able to explain data

Baroni, M.; Costantino, G.; Cruciani, G.; Riganelli, D.; Valigi, R.; Clementi, S. Generating Optimal Linear PLS Estimations (GOLPE): An Advanced Chemometric Tool for Handling 3D-QSAR Problems. *Quant. Struct. Act. Relat.* 1993, 12, 9-20.

Cramer, R. D. III; Bunce, J. D.; Patterson, D. E.; Frank, I. E. Cross validation, bootstrapping and partial least squares compared with multiple regression in conventional QSAR studies. *Quant. Struct. Act. Relat.* 1998, 7, 18-25.

- Training Set Selection
- Molecular Modeling
- Molecular Alignment
- Molecular Interaction Fields
- **Statistical Analysis**
- External Validation
- GRID Plot Interpretation

Standard Deviation Error of Prediction

$$SDEP = \sqrt{\frac{\sum_{i=1}^N (Y_{\text{exp},i} - Y_{\text{pred},i})^2}{N}}$$

Cramer, R. D. III; Bunce, J. D.; Patterson, D. E.; Frank, I. E. Cross validation, bootstrapping and partial least squares compared with multiple regression in conventional QSAR studies. *Quant. Struct. Act. Relat.* **1998**, 7, 18-25.

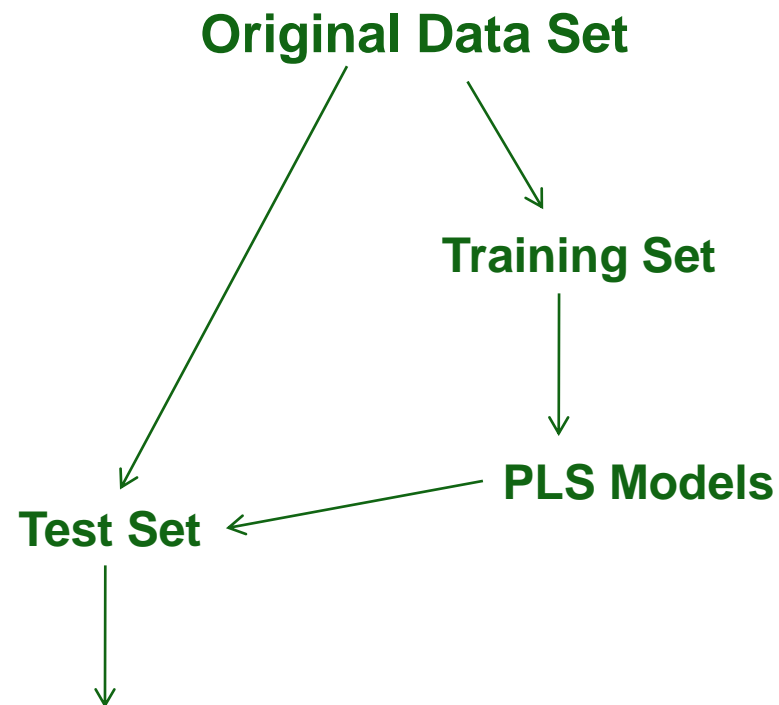
- Training Set Selection
- Molecular Modeling
- Molecular Alignment
- Molecular Interaction Fields
- **Statistical Analysis**
- External Validation
- GRID Plot Interpretation

Squared Predictive Correlation Coefficient

$$q^2 = 1 - \frac{\sum_{i=1}^N (Y_{\text{exp},i} - Y_{\text{pred},i})^2}{\sum_{i=1}^N (Y_{\text{exp},i} - \bar{Y})^2}$$

Cramer, R. D. III; Bunce, J. D.; Patterson, D. E.; Frank, I. E. Cross validation, bootstrapping and partial least squares compared with multiple regression in conventional QSAR studies. *Quant. Struct. Act. Relat.* **1998**, 7, 18-25.

- Training Set Selection
- Molecular Modeling
- Molecular Alignment
- Molecular Interaction Fields
- Statistical Analysis
- **External Validation**
- GRID Plot Interpretation



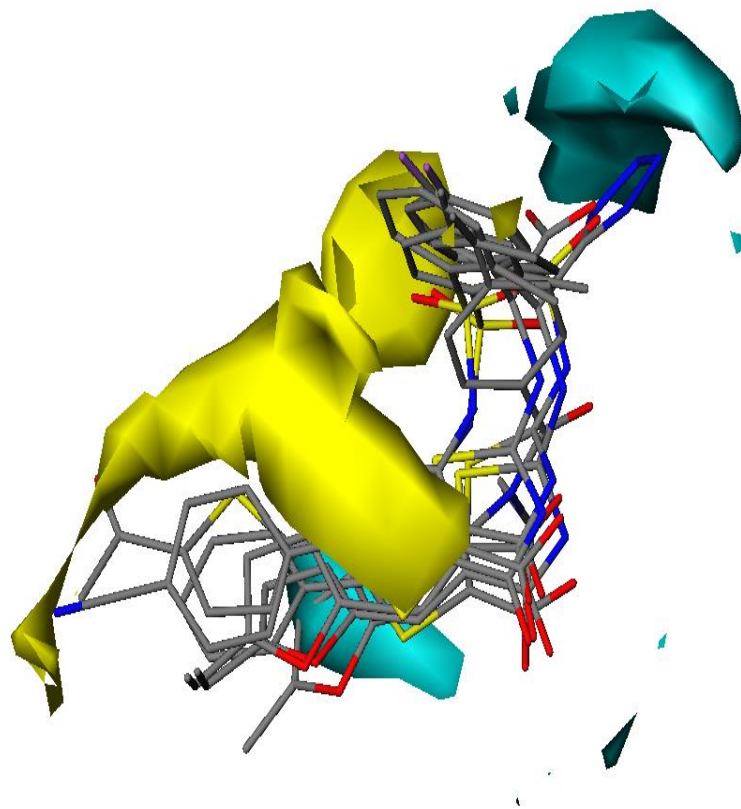
Compare the Test Set Compounds Y_{exp} -values with the Predictions made by the PLS model

Statistical results for (M1-M6) 3D -QSAR global models obtained from diverse GOLPE PLS analysis.

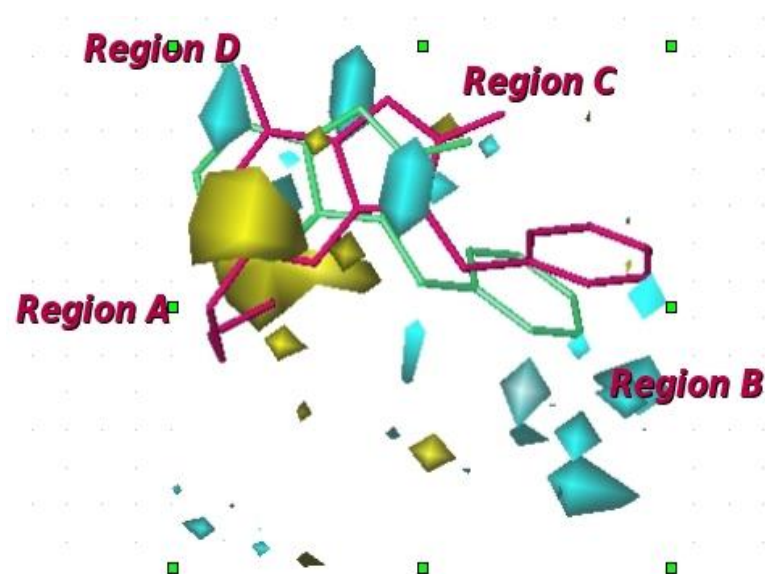
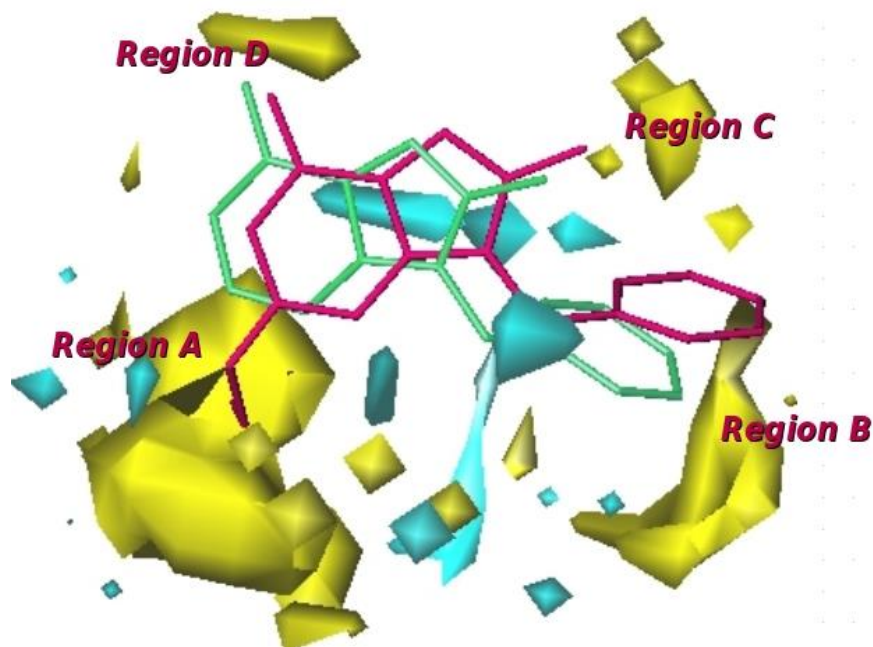
M	P	r^2	LOO			LTO			LSO-5			LHO			Test set
			q^2	SDEP	PC	SDEP _{ext}									
M1	OH2	0.62	0.47	0.71	2	0.46	0.71	2	0.43	0.73	2	0.39	0.76	2	1.08
M2	OH	0.73	0.61	0.61	2	0.61	0.61	2	0.60	0.61	2	0.56	0.64	2	1.05
M3	DRY	0.89	0.64	0.58	5	0.64	0.58	5	0.61	0.60	5	0.55	0.65	5	0.9
M4	N1	0.69	0.58	0.65	2	0.56	0.65	2	0.55	0.65	2	0.52	0.67	2	1.09
M5	O	0.72	0.60	0.61	2	0.60	0.61	2	0.60	0.62	2	0.57	0.64	2	1.05
M6	DRY+ OH	0.70	0.56	0.64	2	0.56	0.64	2	0.55	0.65	2	0.53	0.67	2	1.09

*M: model name; P: GRID probe; LOO: Leave One Out Cross-validation; LTO: Leave Two Out Cross-validation; LSO-5: Leave-Some-Out Cross-validation using 5 groups; LHO: Leave Half Out; r^2 : conventional square correlation coefficient; q^2 : cross-validation correlation coefficient; SDEP: cross-validated standard error of prediction; PC: optimal number of Principal Components; SDEP_{ext}: Standard Error of Prediction for the external test set.

- Training Set Selection
- Molecular Modeling
- Molecular Alignment
- Molecular Interaction Fields
- Statistical Analysis
- External Validation
- **GRID Plot Interpretation**

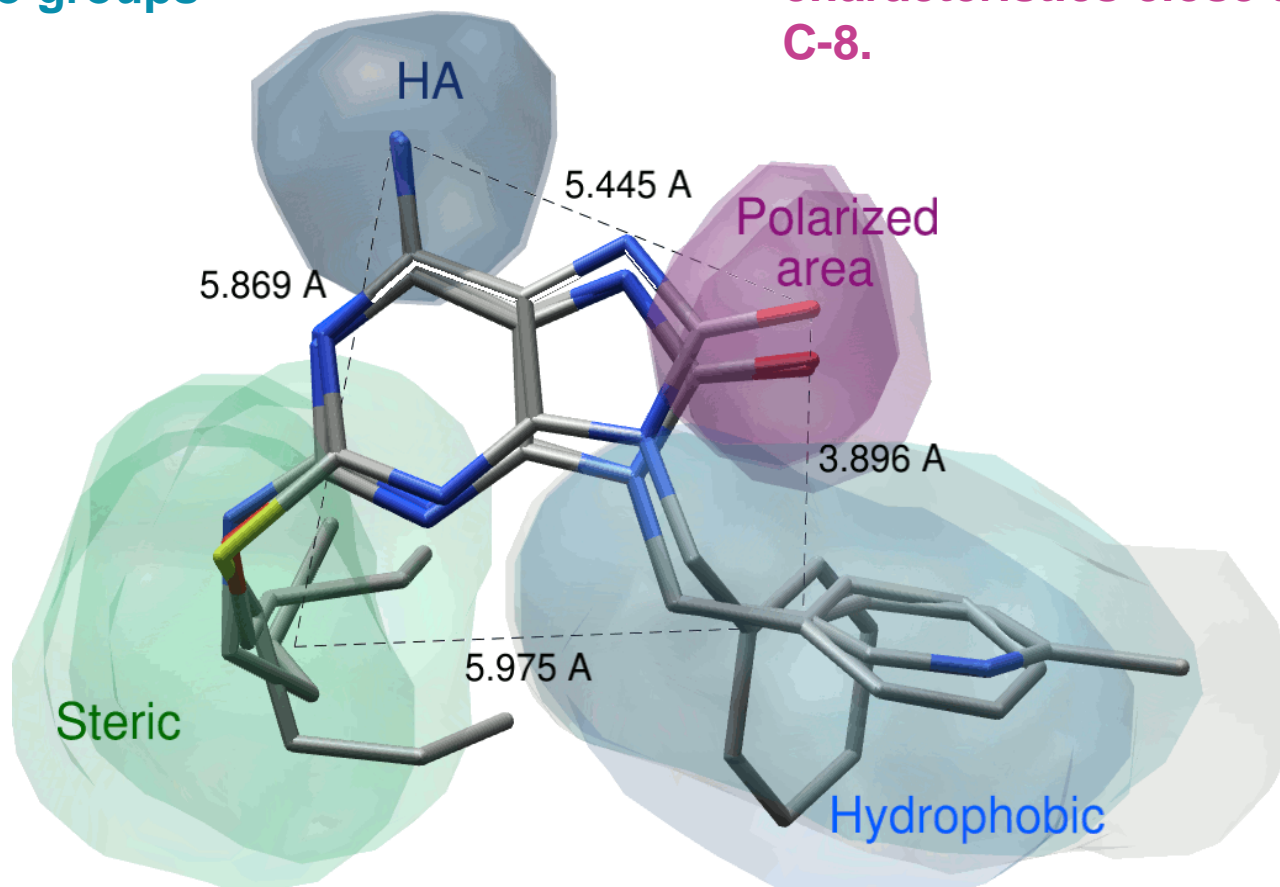


Blue regions	A favorable (negative) interaction INCREASES activity. A unfavorable (positive) interaction DECREASES activity.
Yellow regions	A favorable (negative) interaction DECREASES activity. A unfavorable (positive) interaction INCREASES activity.



GRID/GOLPE PLS Coefficients contour maps for the M2 and M3 3D-QSAR models (contour levels 0.0049 yellow, -0.0049 cyan; contour levels 0.00452 yellow, -0.00452 cyan, respectively). To aid interpretation only the highest active compound **175** (in red) and one of the lowest active compounds **36** (in green) are shown. For the sake of clarity hydrogen atoms are omitted.

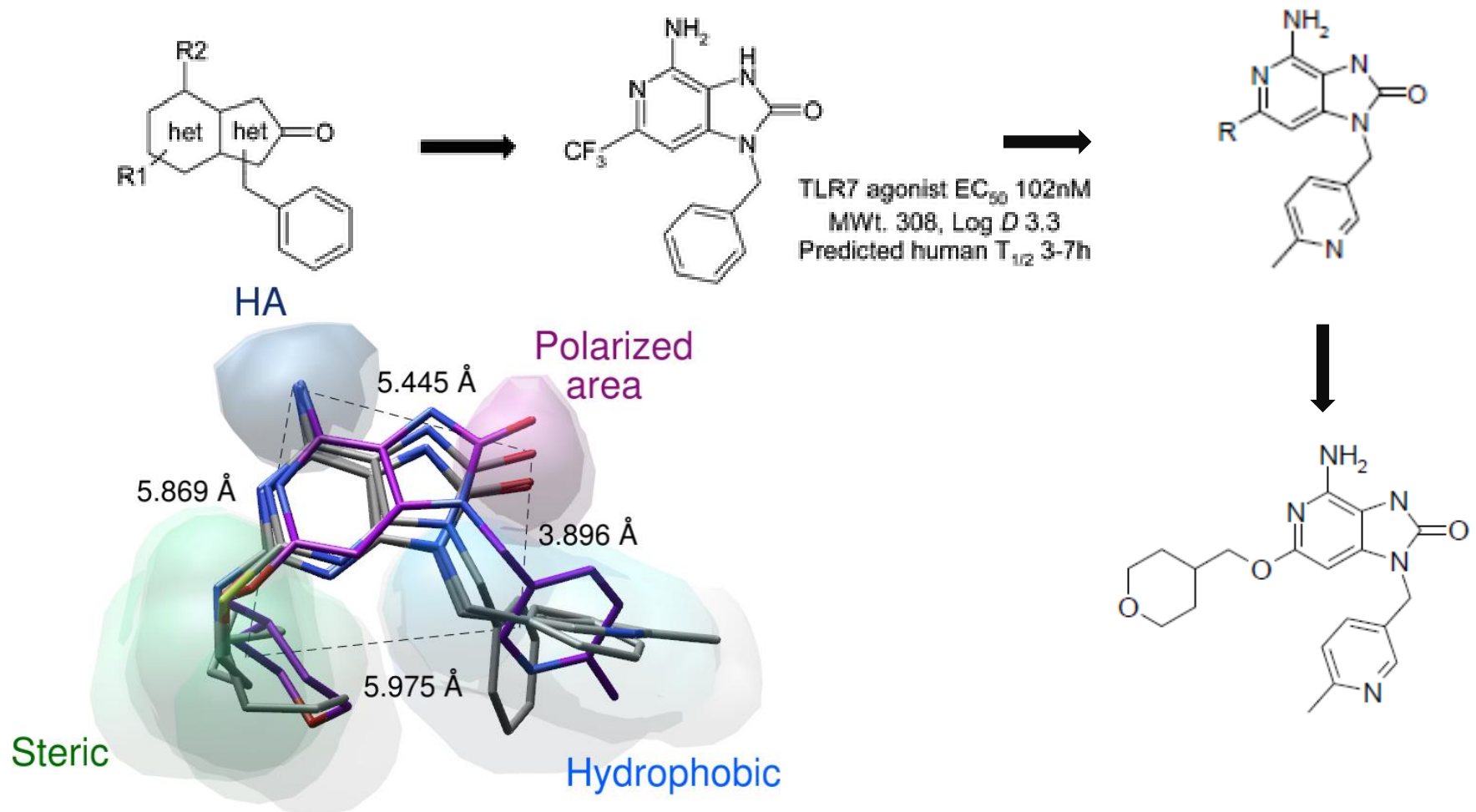
- HA: an acceptor hydrogen bonding region close to the adenine C-6/quinoline C4 amino groups
- Polarized Area: possibly with donator hydrogen bonding characteristics close to adenine C-8.



Musmuca, I.; Simeoni, S.; Caroli, A.; Ragno, R. Small-Molecule Interferon Inducers. Towards the Comprehension of the Molecular Determinants Through Ligand-Based Approaches. *J. Chem. Inf. Model.* **2009**, *49*,1777-1786

Conclusions

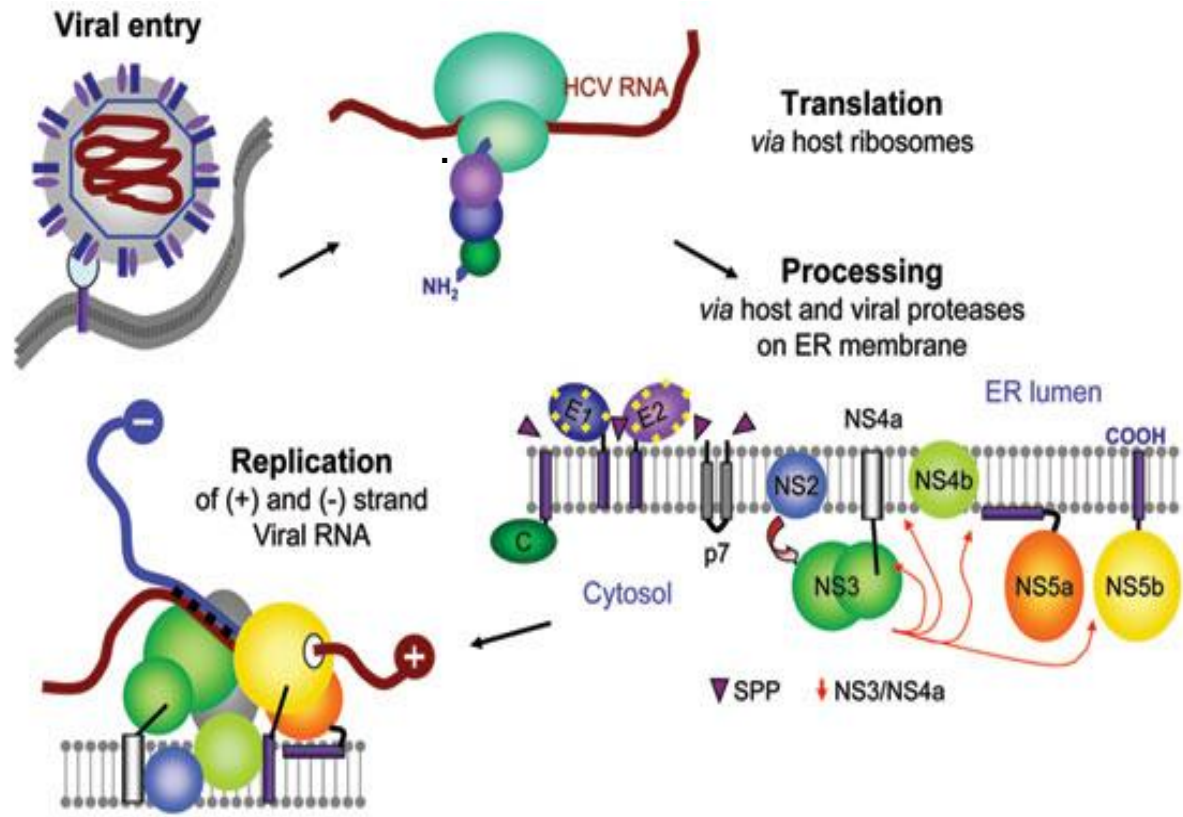
- These features are fully in agreement with several anti-HCV derivatives able to stimulate interferon release in PBMC (peripheral blood mononuclear cell), recently reported by Pryde et al.¹



¹ Pryde et al. The discovery of a novel prototype small molecule TLR7 agonist for the treatment of hepatitis C virus infection *Med. Chem. Commun.*, 2011, Advance Article

HCV NS5B RNA-dependent RNA polymerase

Hepatitis C virus (HCV), the agent responsible for most cases of blood-borne hepatitis, was discovered by Choo et al. 20 years ago¹

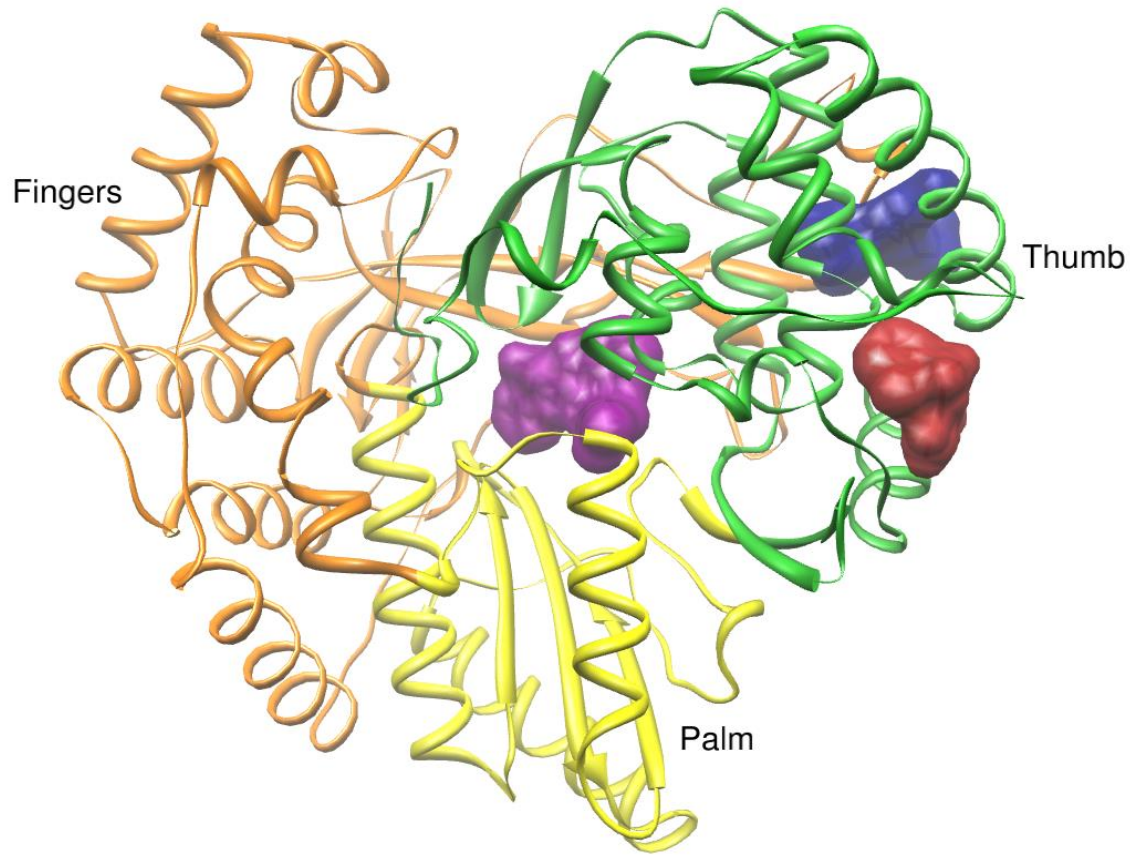


All current treatment protocols for HCV are based upon IFN- α alone or in combination with Ribavirin²

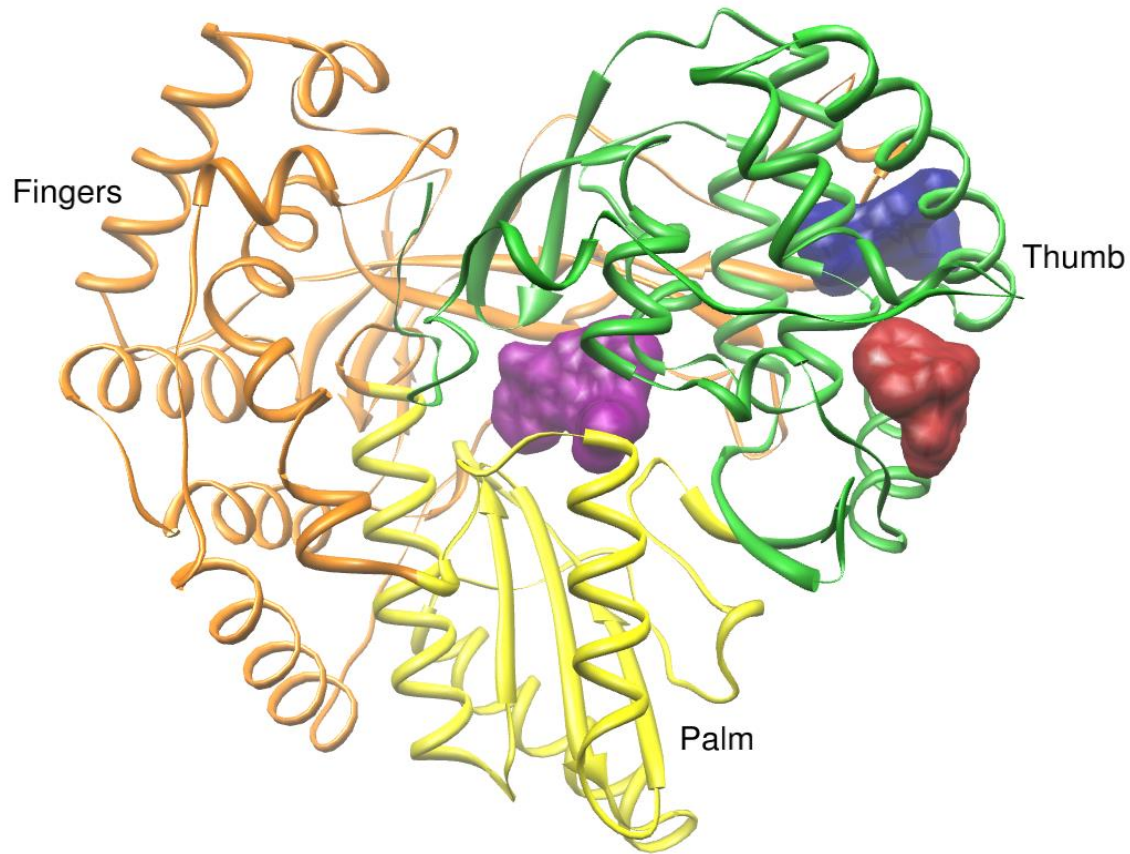
PEG-IFN- α 2a + Ribavirin

¹ Choo, Q.L.; Kuo, G.; Weiner, A. J.; Obverby, L. R.; Bradley, D. W.; Houghton, M. Isolation of a cDNA clone derived from a blood-borne non-A, non-B viral hepatitis genome. *Science* 1989, 244, 359-362.

² Chander, G.; Sulkowski, M. S.; Jenckes, M. W.; Torbenson, M. S.; Bass, H. F. Treatment of chronic hepatitis C: a systematic review. *Hepatology* 2002, 36, S135-S144.



- Essential Enzymatic Activity for a Correct Viral Replication
- Possibility to Design Selective Inhibitors *versus* the Only Infected Cells
- Available Structural Data (Bresanelli et al., *PNAS*, 1999)

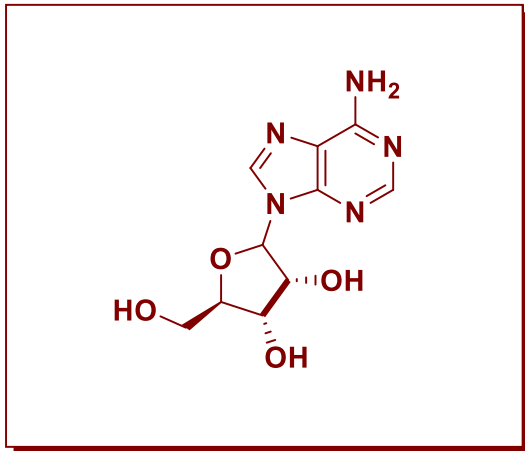


Ribbon show of the overall structure of NS5B RdRp with domains colored according to thumb (green), palm (yellow), and fingers (orange). Three allosteric binding sites surfaces are also shown. Dark red colored surface corresponds to the thumb allosteric bs, dark violet colored surface corresponds to the palm allosteric bs and the dark blue colored surface corresponds to the allosteric binding site situated in the thumb domain, near but clearly distinct from the first one (dark red surface).

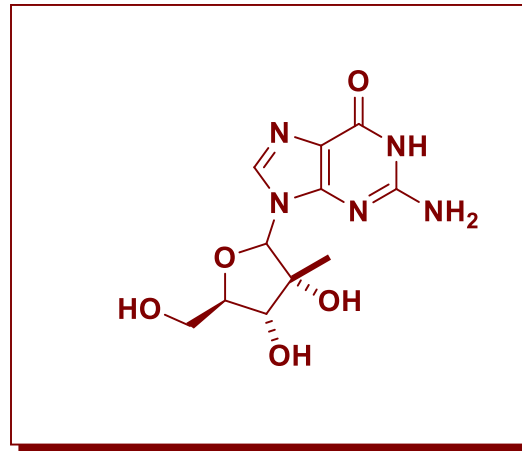
NS5B Inhibitors can be classified into two major groups:

Nucleoside Analogues

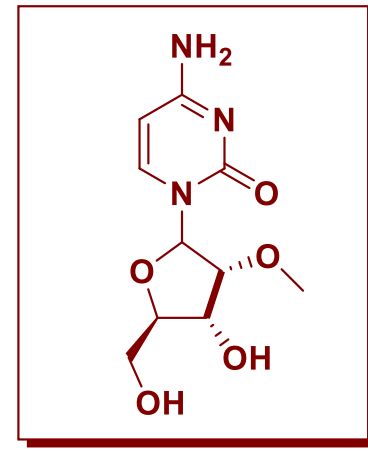
Non Nucleoside Analogues



2'-C-methyladenosine

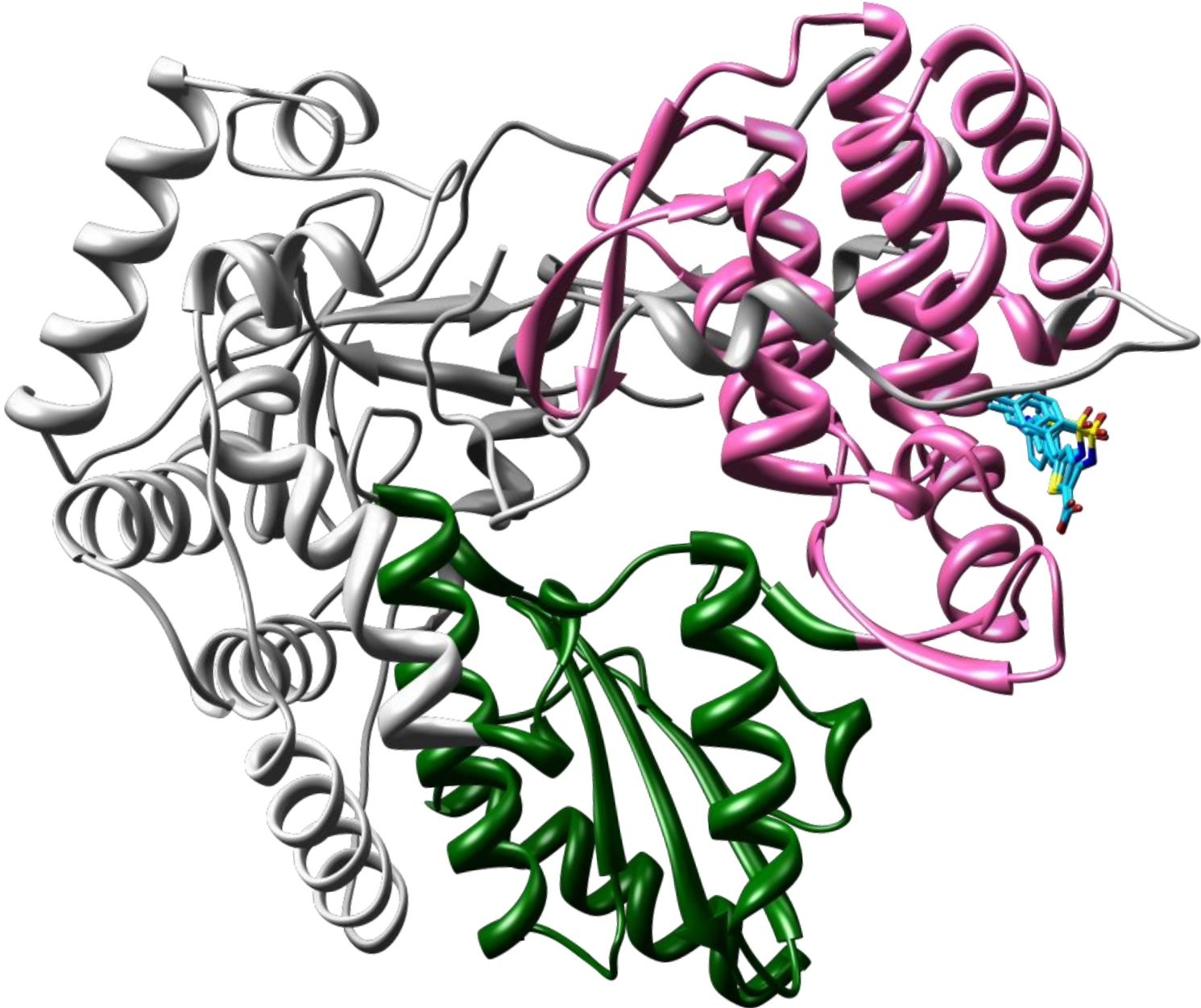


2'-C-methylguanosine

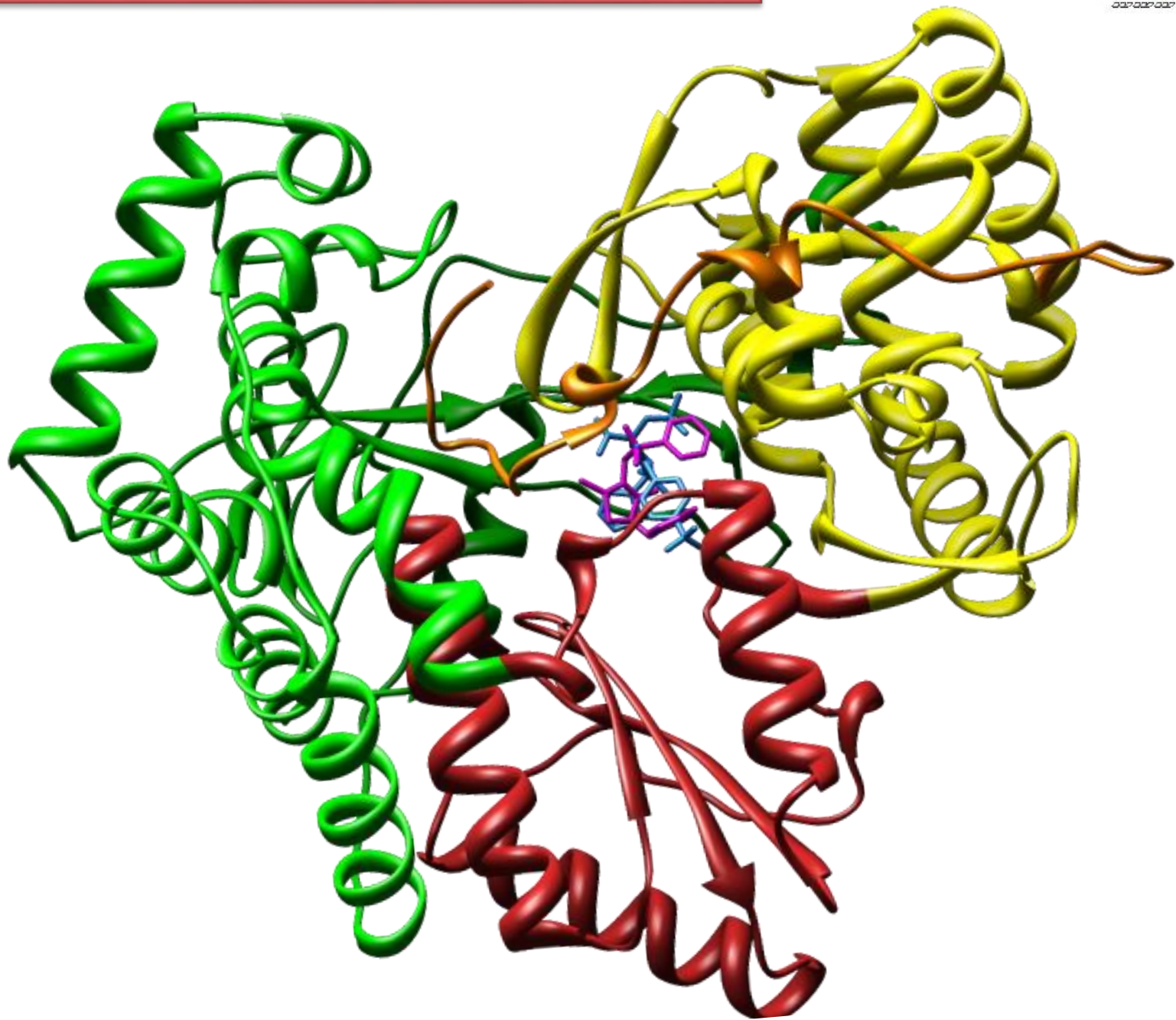


2'-O-methylcytidine

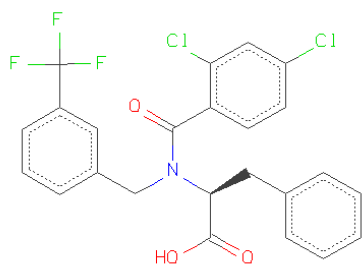
Thumb Allosteric Inhibitors



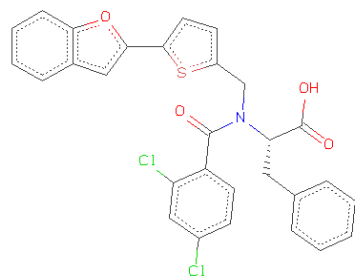
Palm Allosteric Inhibitors



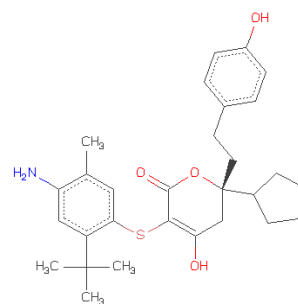
Ligand-Based, Structure-Based and 3D-QSAR Protocol



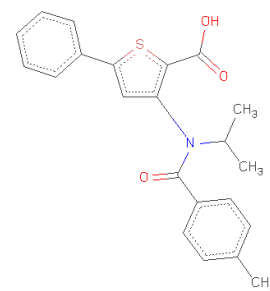
1nhu



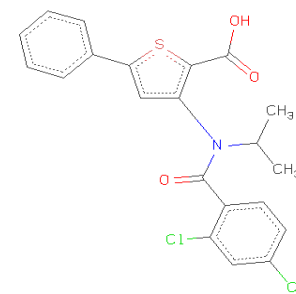
1nhv



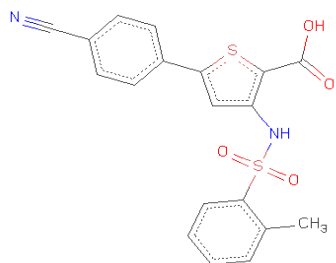
1os5



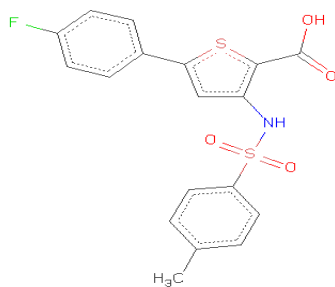
1yvz



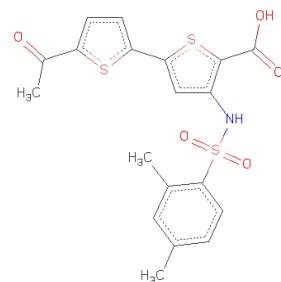
1yvz



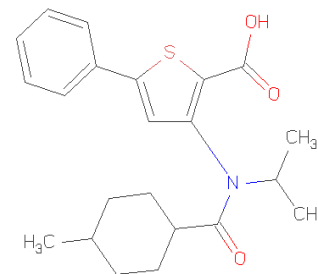
2d3u



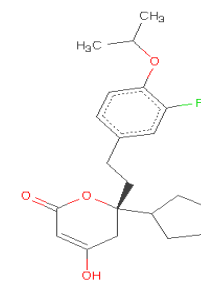
2d3z



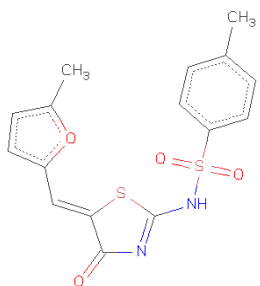
2d41



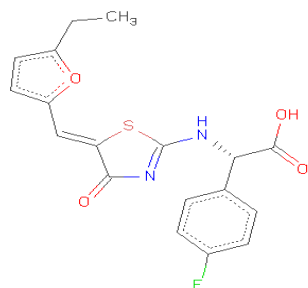
2gir



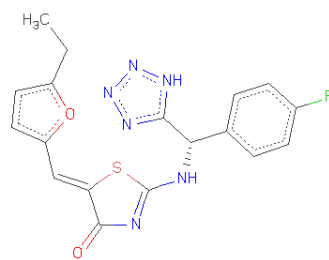
2hai



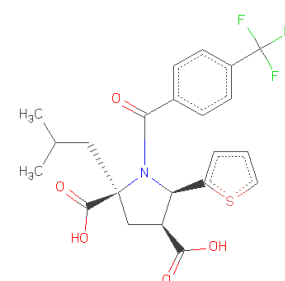
2hwh



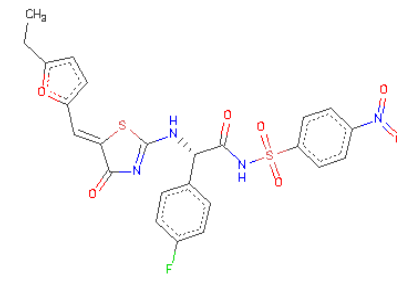
2hwi



2i1r

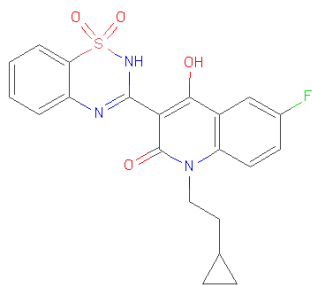


2jc0

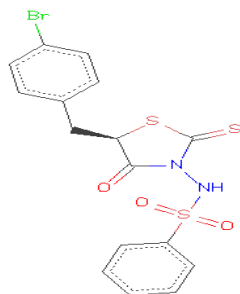


2o5d

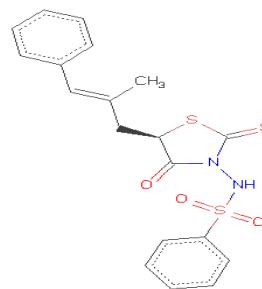
Ligand-Based, Structure-Based and 3D-QSAR Protocol



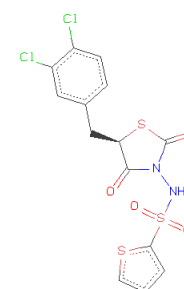
2giq



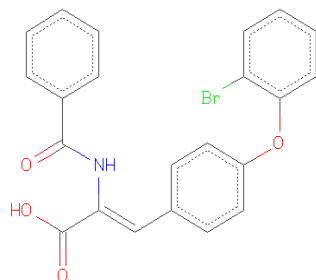
2awz



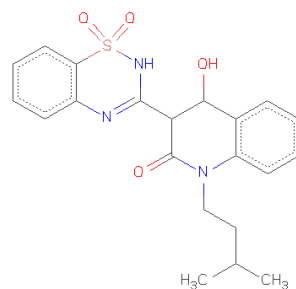
2ax0



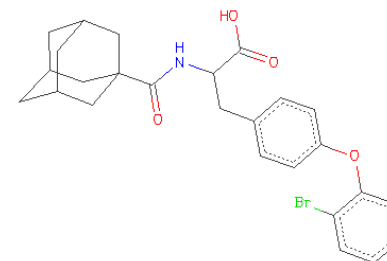
2ax1



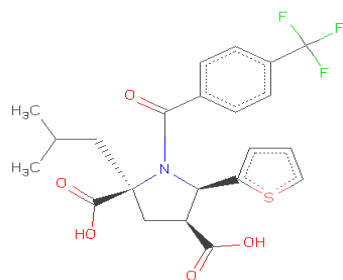
1yvf



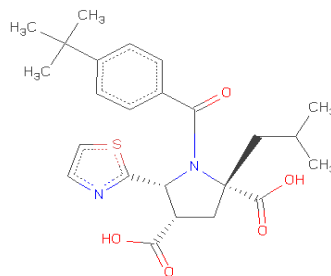
2fvc



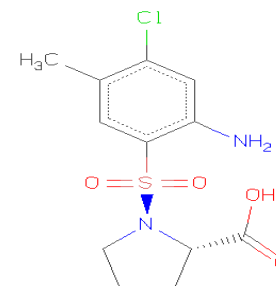
1z4u



2jc0

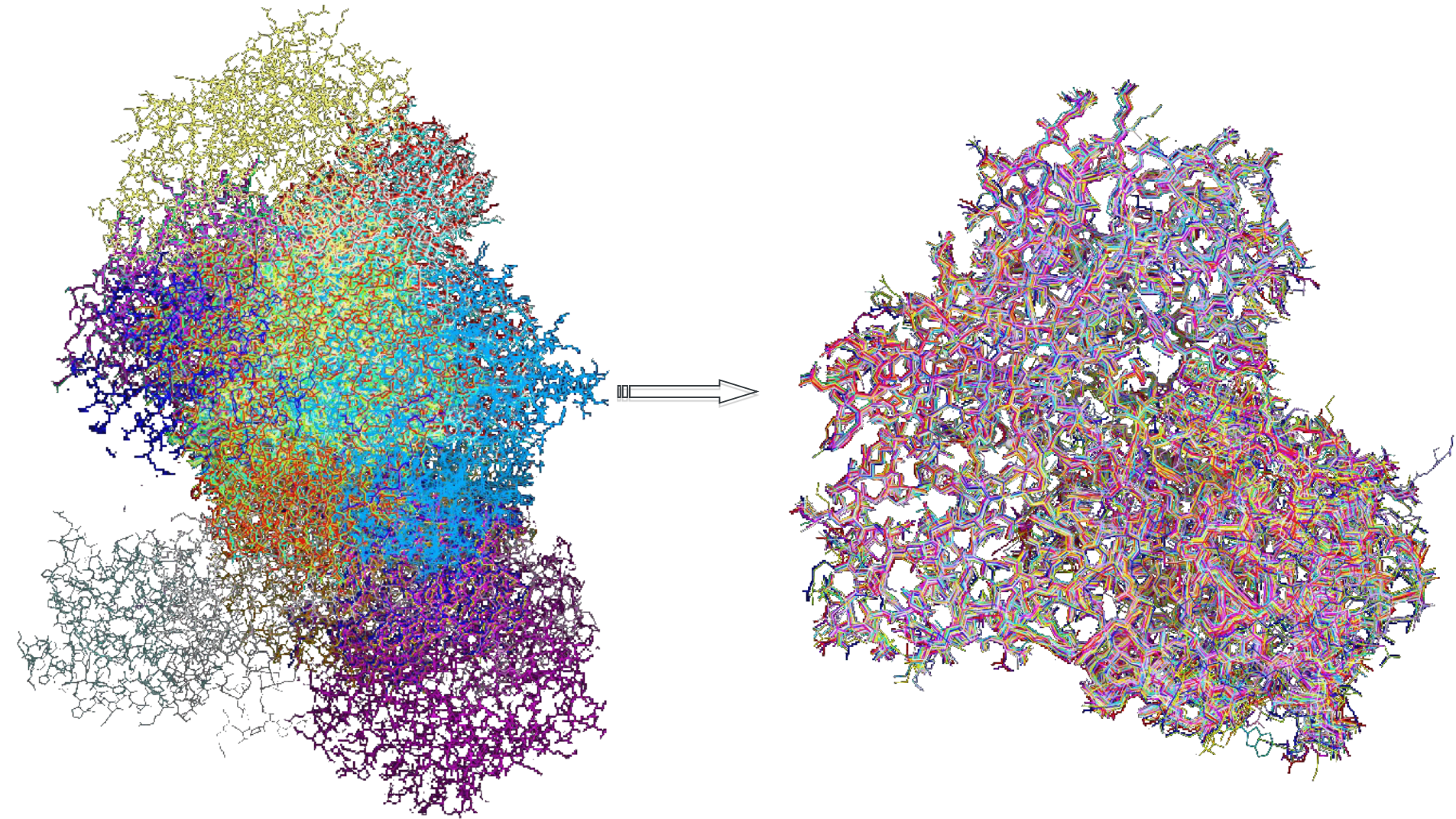


2jc1



2gc8

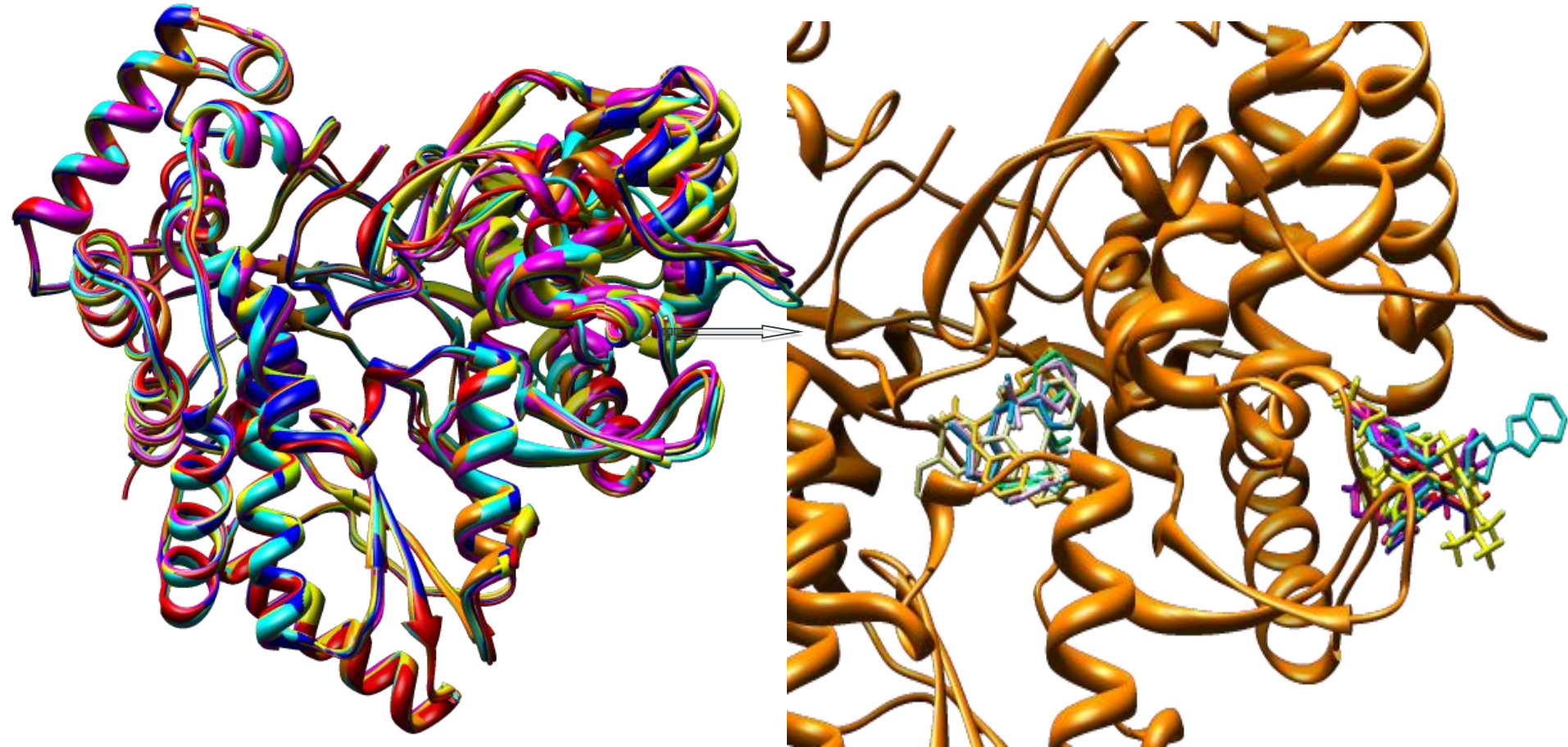
Polymerase-Inhibitor Complex Structures Preparation



Case et al. The Amber biomolecular simulation programs. *J. Comput. Chem.* **2005**, 26, 1668-1688

Meng, E. C.; Pettersen, E. F.; Couch, G. S.; Huang, C. C.; Ferrin, T. E. Tools for integrated sequence-structure analysis with UCSF Chimera. *BMC Bioinformatics* **2006**, 7, 339.

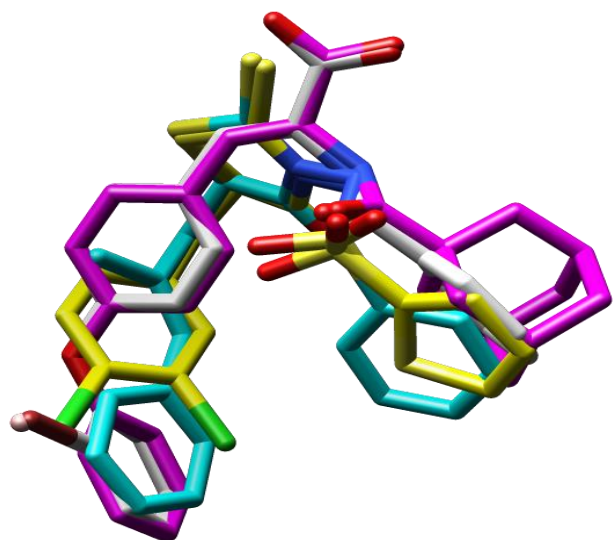
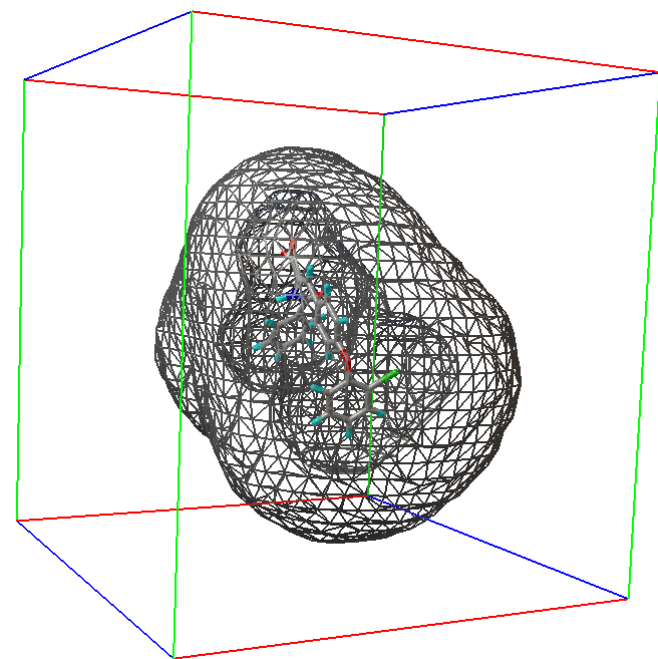
Polymerase-Inhibitor Complex Structures Preparation



Molecular Interaction Fields



GRID/GOLPE

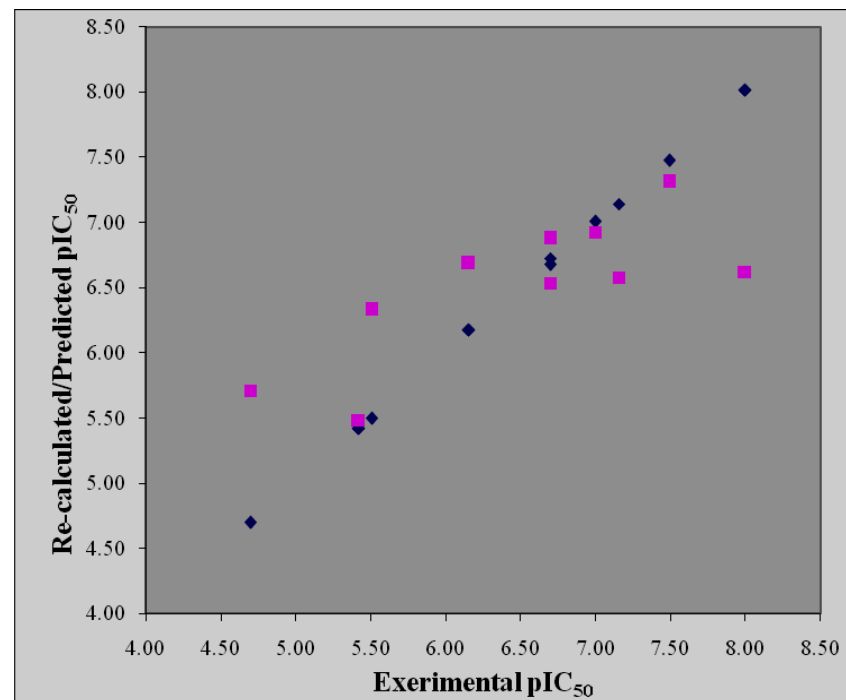
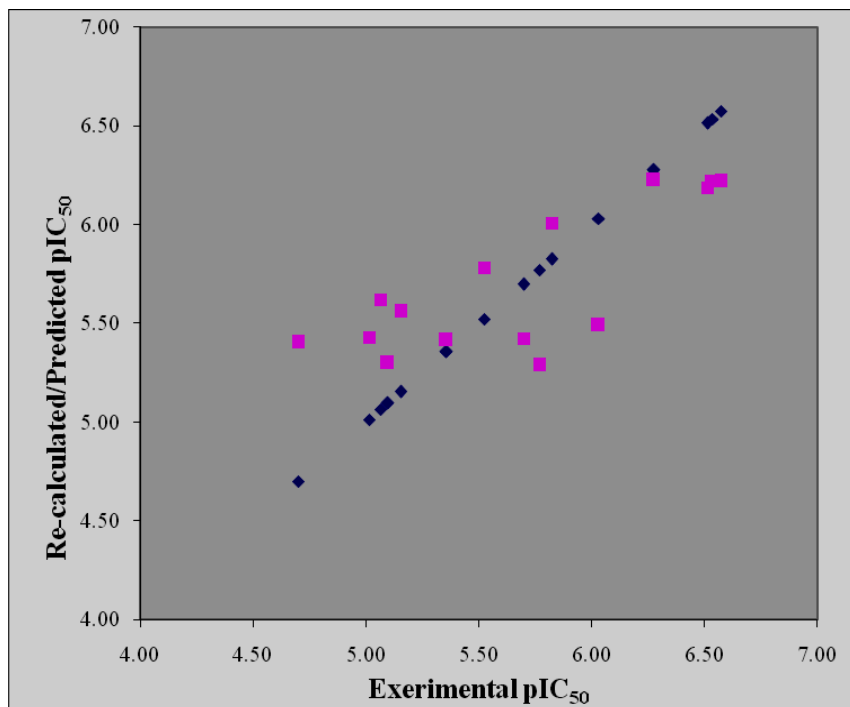


2 Structure-Based 3D-QSAR Models

PLS Analysis Results for the Thumb and the Palm Structure-Based 3D-QSAR Models.^a

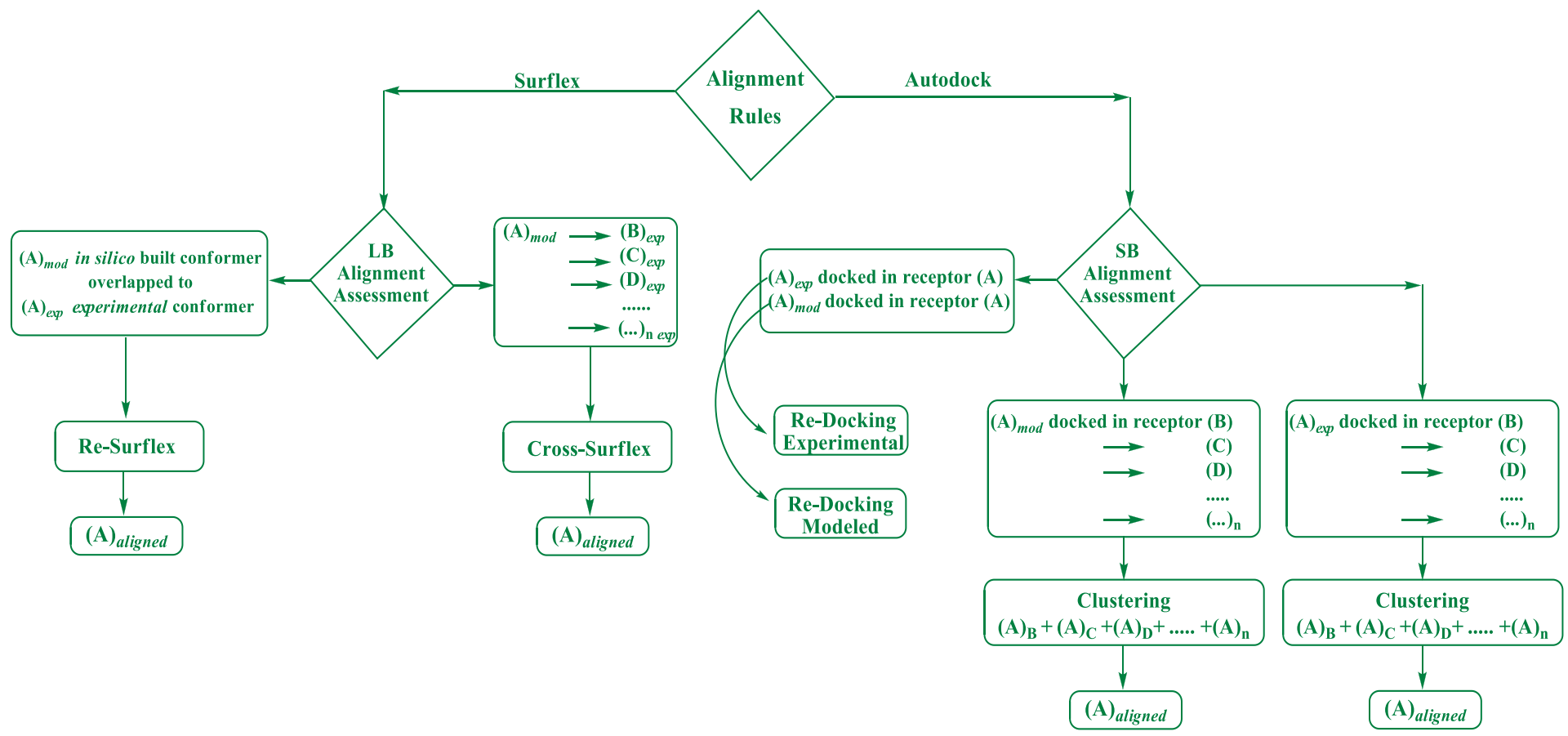
<i>N</i>	GRID Probe	<i>V</i>	PC	<i>r</i> ²	<i>q</i> ²
15	C1=	5133	3	0.99	0.69
10	C1=	3848	3	0.99	0.55

^a *N*, number of compounds in the training set; *V*, number of GOLPE variables; PC, optimal number of principal components; *r*², conventional square correlation coefficient; *q*², cross-validation correlation coefficient; SDEP, cross-validated standard error of prediction using the leave-five-out cross-validation method



Fitting and Cross-Validation Plots for the Thumb (left) and Palm (right) Training Sets.

Key Steps for the Assessment of SB and LB Alignments Processes



Assessment of Docking: Redocking

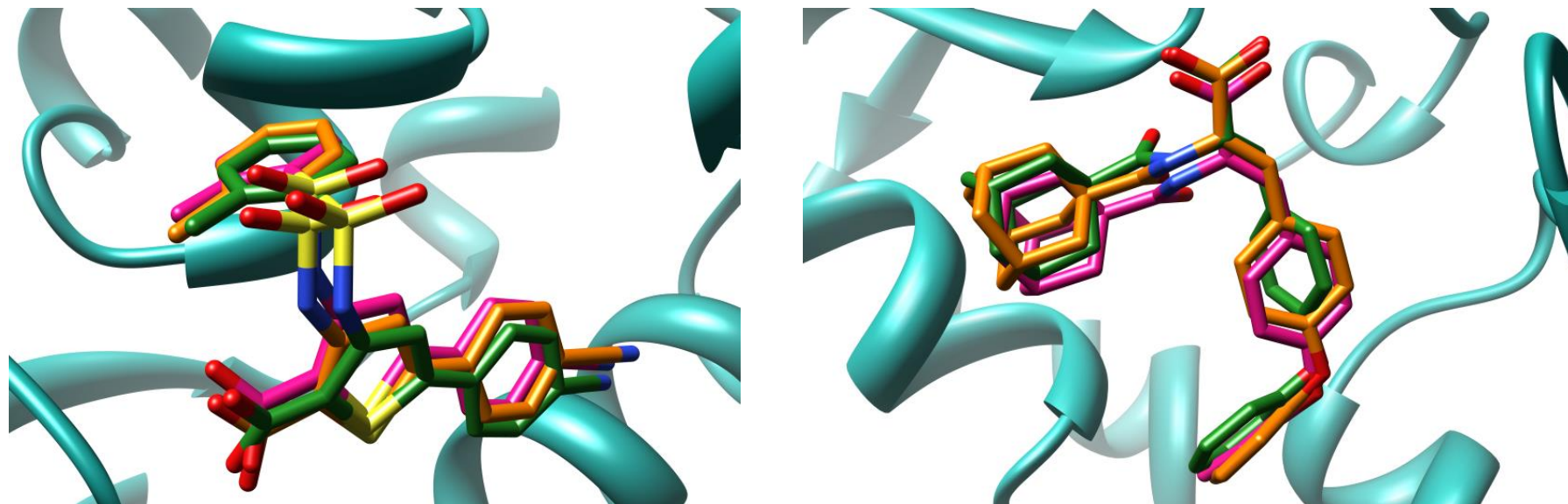
Assessment of the Autodock Program in the Redocking Stage. RMSD Values for the First Ranked Pose (Best Docked), the Lowest Energy Docked Conformation of the Most Populated Cluster, (Best Cluster) and the One Closest to the Experimentally Bound Conformation (Best Fitted Cluster).

Binding Site	PDB	Ligand Entry	Best Docked		Best Cluster		Best Fitted	
			RMSD	Cluster N°	RMSD	Cluster N°	RMSD	
Thumb	1NHU	1	3.17	3	2.17	3	0.89	
	1NHV	2	4.13	2	4.75	26	1.86	
	1OS5	13	3.46	1	3.46	9	1.50	
	1YVX	3	3.81	1	3.81	6	1.58	
	1YVZ	4	3.74	4	1.92	4	0.78	
	2D3U	6	0.71	1	0.71	1	0.44	
	2D3Z	7	0.75	1	0.75	1	0.60	
	2D41	8	1.43	1	1.43	1	0.58	
	2GIR	5	5.70	2	1.12	2	0.70	
	2HAI	14	2.05	1	2.05	1	0.92	
	2HWH	9	9.86	2	2.13	2	0.79	
	2HWI	10	0.34	1	0.34	1	0.24	
	2I1R	11	5.84	2	1.67	2	0.73	
	2JC0	15	0.85	1	0.85	1	0.68	
	2O5D	12	5.74	3	2.78	7	1.28	
Average RMSD			3.44		2.00		0.90	
Palm	1YVF	17	3.38	4	1.12	4	0.93	
	1Z4U	16	0.89	1	0.89	1	0.57	
	2AWZ	18	3.53	3	1.72	3	1.11	
	2AX0	19	0.84	1	0.84	1	0.52	
	2AX1	20	3.24	2	0.99	2	0.61	
	2FVC	21	1.04	1	1.04	1	0.74	
	2GC8	24	2.03	1	2.03	2	1.82	
	2GIQ	22	3.49	5	1.91	5	1.81	
	2JC0	15	0.65	1	0.65	1	0.42	
	2JC1	23	0.74	1	0.74	1	0.47	
	Average RMSD			1.98		1.19		0.90

Assessment of Docking: Redocking Modeled

Checks more realistically Autodock's ability to reproduce binding mode conformations of molecules with no experimental binding data

Examples of Redocking Modeled



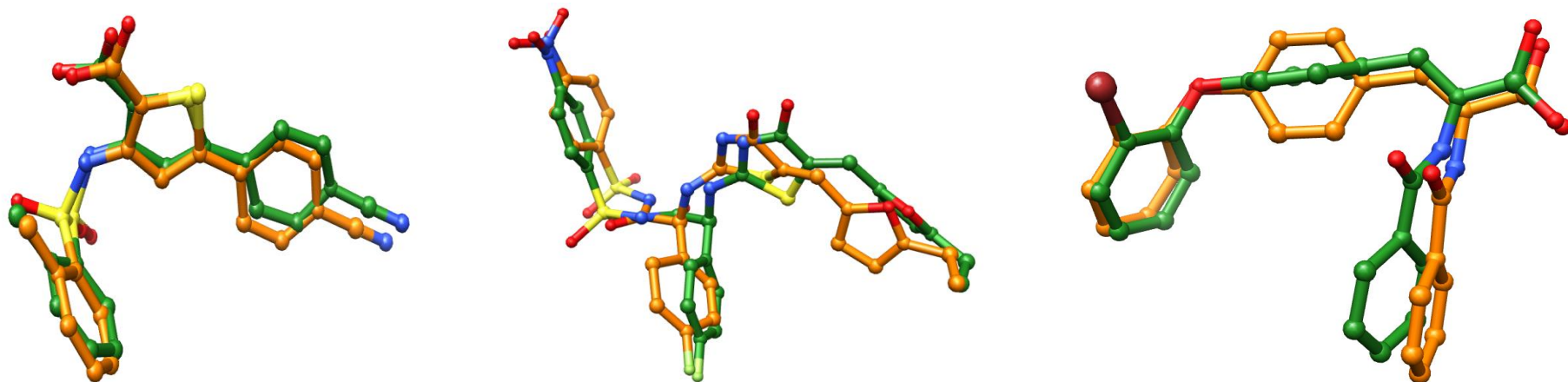
Superimposition of the Surflex-aligned conformer (carbon atoms in green) and the re-docked conformer (carbon atoms in magenta) to the experimental conformation (in orange) of one thumb NNI (**6**, on the left) and one palm NNI (**16**, on the right) within the NS5B (cyan colored ribbons). Atom bonds are in stick fashion. Hydrogen atoms are omitted for the sake of clarity.

Assessment of Docking: Cross-Docking

binding site	PDB	ligand entry	best docked (rmsd)	best cluster		best fitted cluster		
				cluster N ^o	rmsd	cluster N ^o	rmsd	
thumb	1NHU	1	2.25	1	2.25	3	1.87	
	1NHV	2	4.37	14	3.68	19	2.54	
	1OS5	13	7.59	5	3.61	32	1.81	
	1YVX	3	3.51	2	1.77	10	1.58	
	1YVZ	4	1.73	1	1.73	1	1.67	
	2D3U	6	5.79	2	5.06	14	1.79	
	2D3Z	7	5.36	2	3.75	8	1.22	
	2D4I	8	6.49	2	1.51	2	1.51	
	2GIR	5	1.57	1	1.57	1	1.57	
	2HAI	14	1.45	1	1.45	1	1.45	
	2HWH	9	3.60	7	2.9	7	1.71	
	2HWI	10	3.61	3	2.20	13	1.40	
	2HIR	11	2.27	2	1.77	3	1.61	
	2JC0	15	4.26	11	9.7	3	3.38	
	2O5D	12	3.48	1	3.48	18	1.73	
	average rmsd			3.82		3.1		1.79
palm	1YVF	17	2.56	2	3.43	9	2.52	
	1Z4U	16	2.26	2	3.87	12	1.78	
	2AWZ	18	1.64	1	1.64	1	1.64	
	2AX0	19	1.85	1	1.85	3	1.58	
	2AXI	20	1.68	1	1.68	1	1.68	
	2FVC	21	1.88	1	1.88	3	1.06	
	2GC8	24	11.13	2	2.08	6	1.84	
	2GIQ	22	1.84	1	1.84	11	1.64	
	2JC0	15	1.21	1	1.21	1	1.21	
	2JC1	23	0.97	1	0.97	1	0.97	
	average rmsd			2.7		2.09		1.59

Ligand-Based Alignment: Surfex-Assessment

1. The Ligand-Based alignment of the molecules was achieved using Surfex-Sim
2. This method optimizes the pose of a query molecule to an object molecule in order to maximize 3D similarity



Examples of Surfex alignment. Superimposition of the modeled ligand conformations (carbon atoms in green) to the experimental ones (carbon atoms in orange) of three compounds of training sets (from left to right, compounds **6**, **12** and **16**). Atom bonds are in ball and stick fashion. Hydrogen atoms are omitted for the sake of clarity.

TEST SET {
 Thumb Domain (81 molecules)
 Palm Domain (223 molecules)

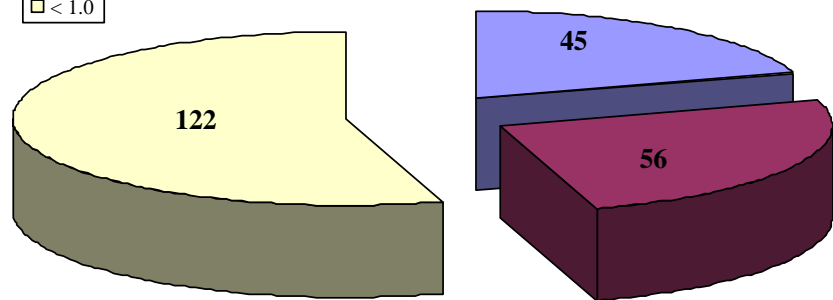
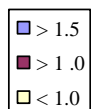
PLS Analysis Results for the Thumb and the Palm Structure-Based 3D-QSAR Models.^a

<i>N</i>	GRID Probe	<i>V</i>	PC	<i>r</i> ²	<i>q</i> ²	SDEP _{ext}
15	C1=	5133	3	0.99	0.69	0.65
10	C1=	3848	3	0.99	0.55	1.05

^a *N*, number of compounds in the training set; *V*, number of GOLPE variables; PC, optimal number of principal components; *r*², conventional square correlation coefficient; *q*², cross-validation correlation coefficient; SDEP, cross-validated standard error of prediction using the leave-five-out cross-validation method

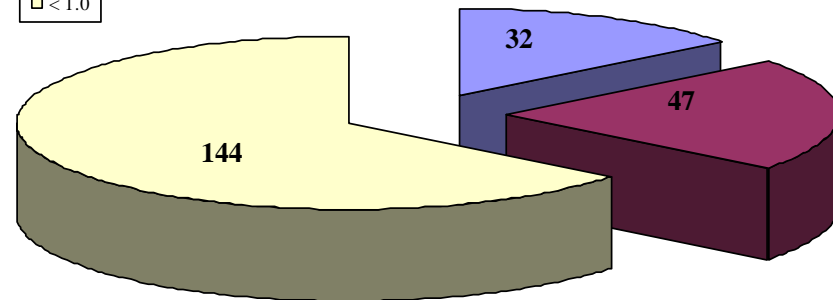
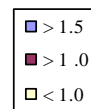
External Validation of the 3D-QSAR Models

Palm Prediction Surfex Alignment



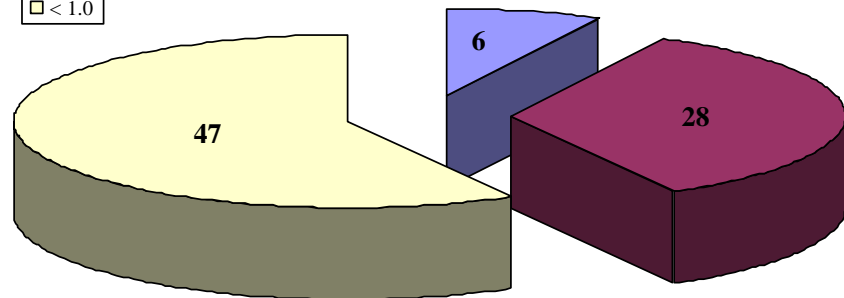
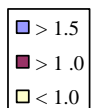
Total number of cpds: 223

Palm Prediction Autodock Alignment



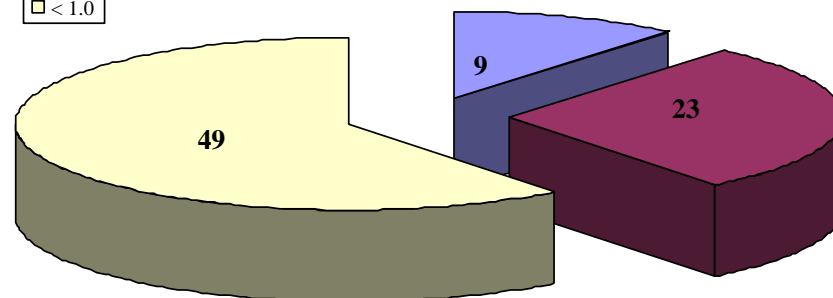
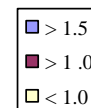
Total number of cpds: 223

Thumb Prediction Surfex Alignment



Total number of cpds: 81

Thumb Prediction Autodock Alignment



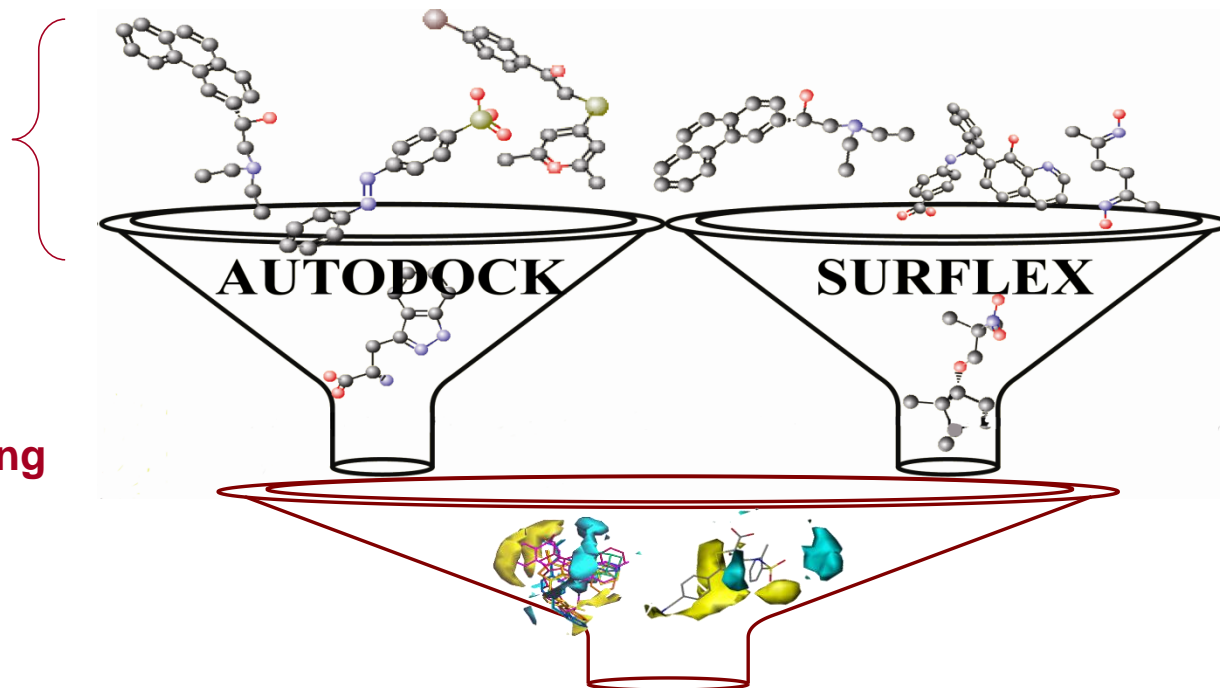
Total number of cpds: 81

Virtual Screening

NCI Diversity Set
(about 1990 mols)

Structure – Based
and Ligand - Based Filtering

3D – QSAR
Re - scoring



20 candidates for the Thumb Domain



2 molecules

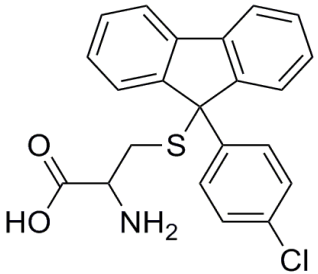
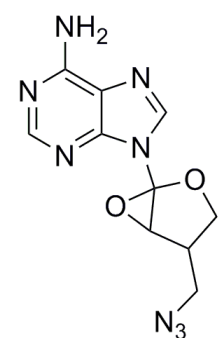
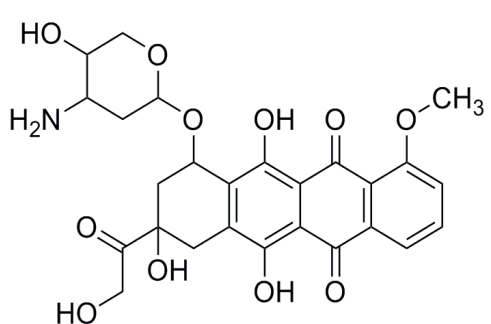
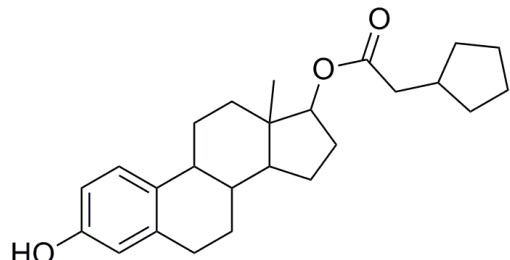
20 candidates for the Palm Domain



2 molecules

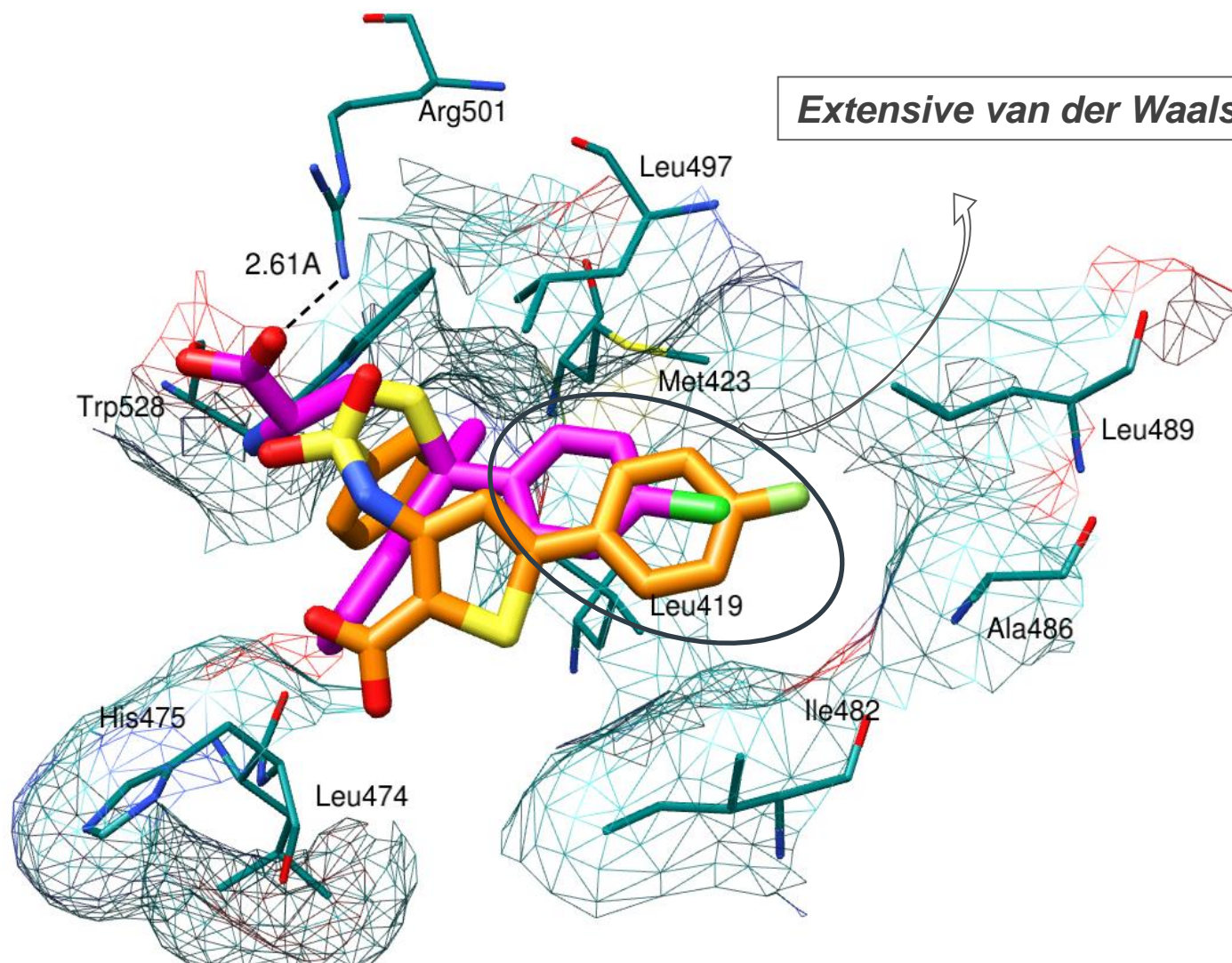
Virtual Screening

Molecular Structure and Antiviral Activity^a of the Compounds Selected by VS Protocol

Thumb Domain		Palm Domain	
			
NSC 123526	NSC 125626	NSC 169534	NSC 3354
$IC_{50} = 46.0 \mu M$	$IC_{50} = 73.3 \mu M$	$IC_{50} = 64.5 \mu M$	$IC_{50} = 54.3 \mu M$

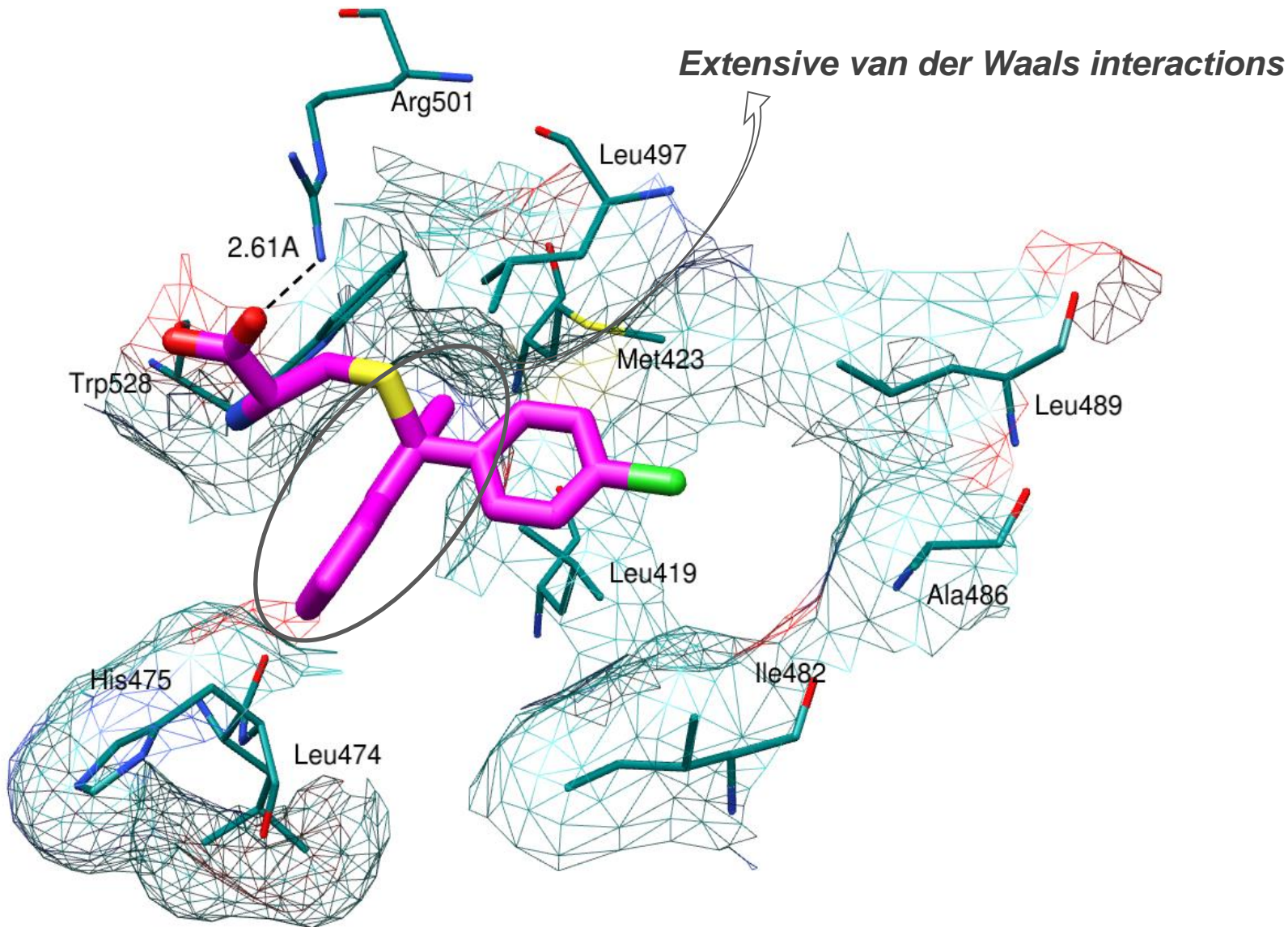
^aThe data represents an average of at least two independent experiments

Binding Mode Analysis



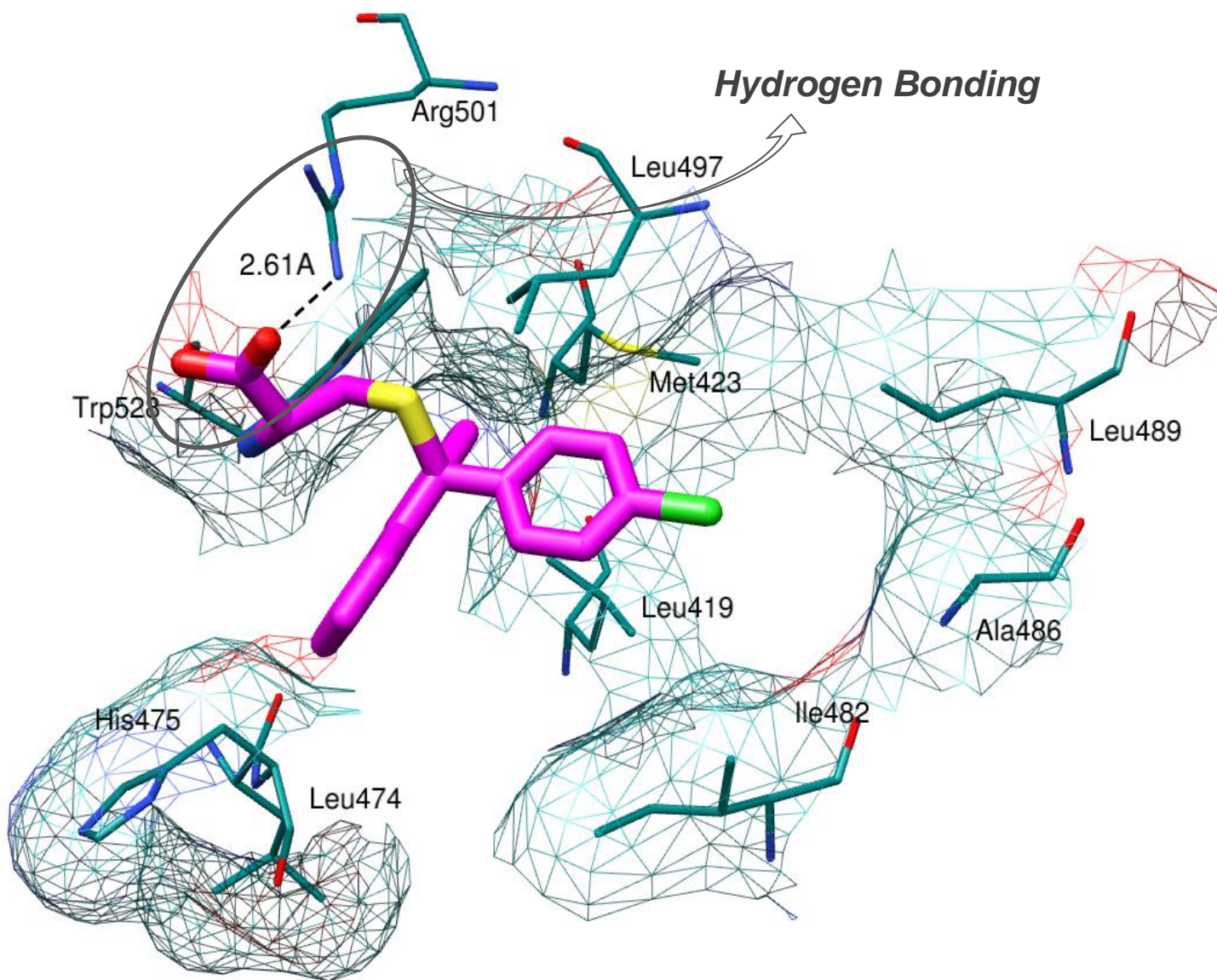
Musmuca, I.; Caroli, A.; Mai, A.; Kaushik-Basu, N.; Arora, P. and Rino Ragno. Combining Structure-Based Three-Dimensional Quantitative Structure-Activity Relationship Analysis and Cross-Docking Procedures for in Silico Screening of Hepatitis C Virus NS5B Polymerase Inhibitors. *J. Chem. Inf. Model.* **2010**, *50*, 662-676.

Binding Mode Analysis



Musmuca, I.; Caroli, A.; Mai, A.; Kaushik-Basu, N.; Arora, P. and Rino Ragno. Combining Structure-Based Three-Dimensional Quantitative Structure-Activity Relationship Analysis and Cross-Docking Procedures for in Silico Screening of Hepatitis C Virus NS5B Polymerase Inhibitors. *J. Chem. Inf. Model.* **2010**, *50*, 662-676.

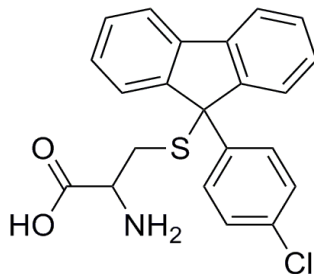
Binding Mode Analysis



Musmuca, I.; Caroli, A.; Mai, A.; Kaushik-Basu, N.; Arora, P. and Rino Ragno. Combining Structure-Based Three-Dimensional Quantitative Structure-Activity Relationship Analysis and Cross-Docking Procedures for in Silico Screening of Hepatitis C Virus NS5B Polymerase Inhibitors. *J. Chem. Inf. Model.* **2010**, *50*, 662-676.

Virtual Screening Results

- Virtual Screening of 1990 compounds from the NCI Diversity Set
- Structure-Based 3D-QSAR models used as external scoring function
- Selection of the most predictive molecules for biological assays against recombinant NS5BC Δ 21
- Outcome of biological studies: 4 active compounds versus our biological target
- Binding mode analysis of 4 selected compounds within thumb subdomain
- Selection of NSC 123526 as our hit compound since:
 - i. Endowed with the lowest inhibitory activity ($IC_{50} = 46.0 \mu M$)
 - ii. Its docked conformer, best overlaps with the most active compound of the thumb training set (visual inspection of their binding modes)
 - iii. The most interesting from a medicinal chemistry point of view



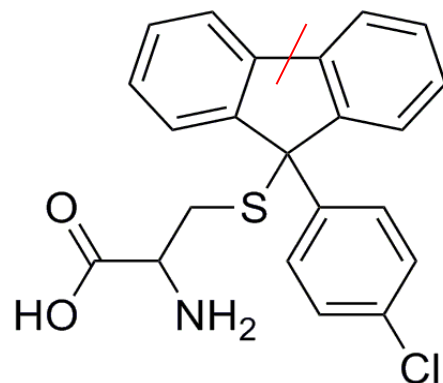
Literature

Hit
Structural
Considerations

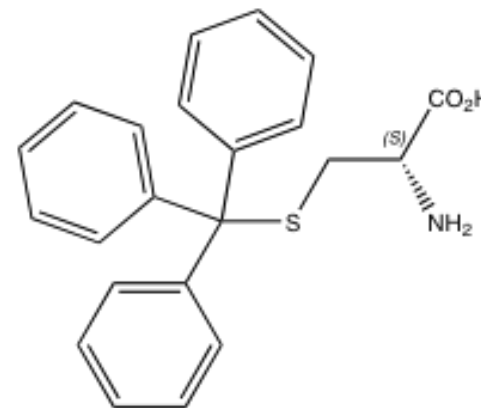
Keeping the most
important interactions

Synthetic Feasibility

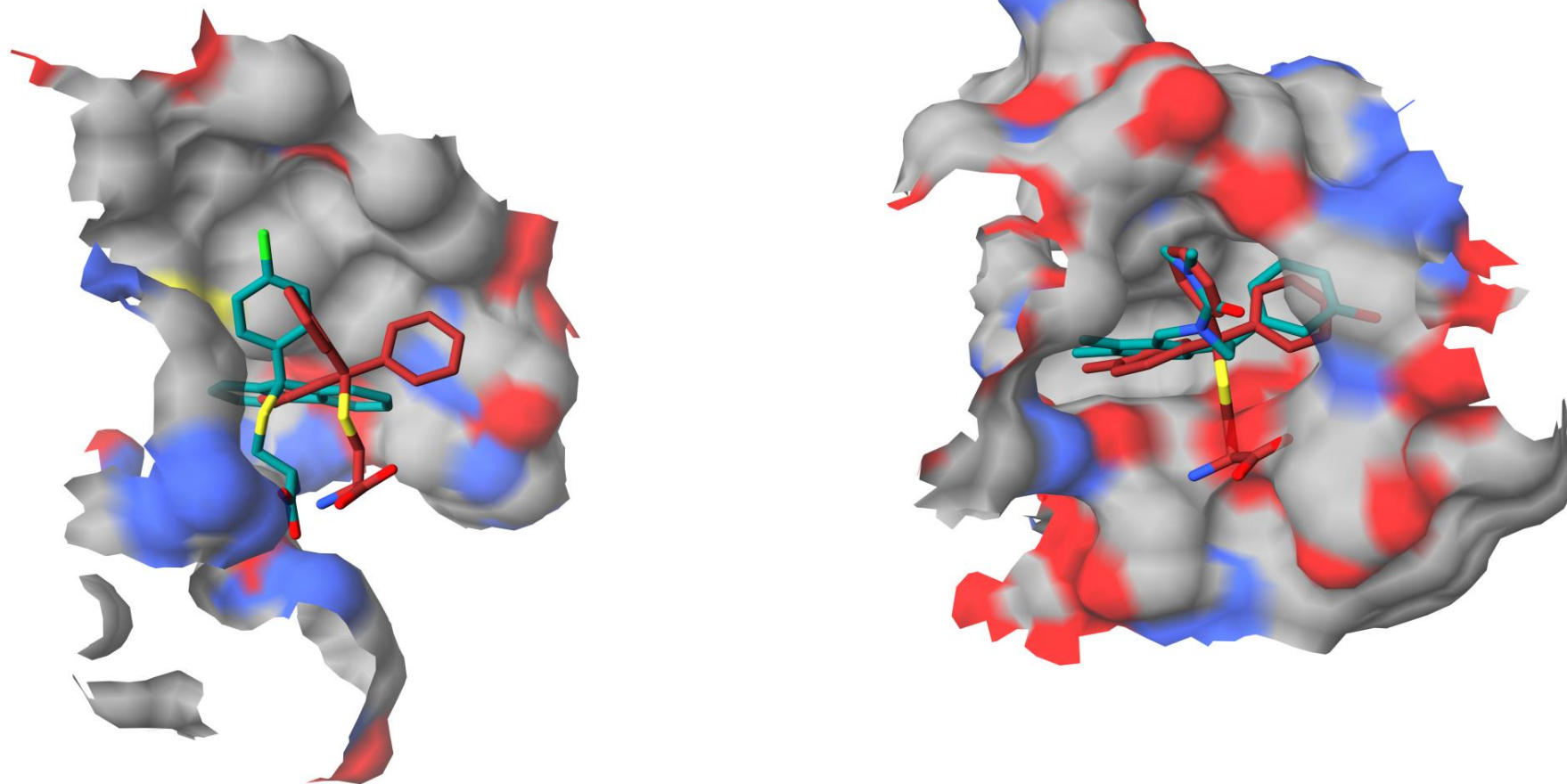
Constrained Derivative of a *S*-Trityl -L-Cysteine



NSC 123526

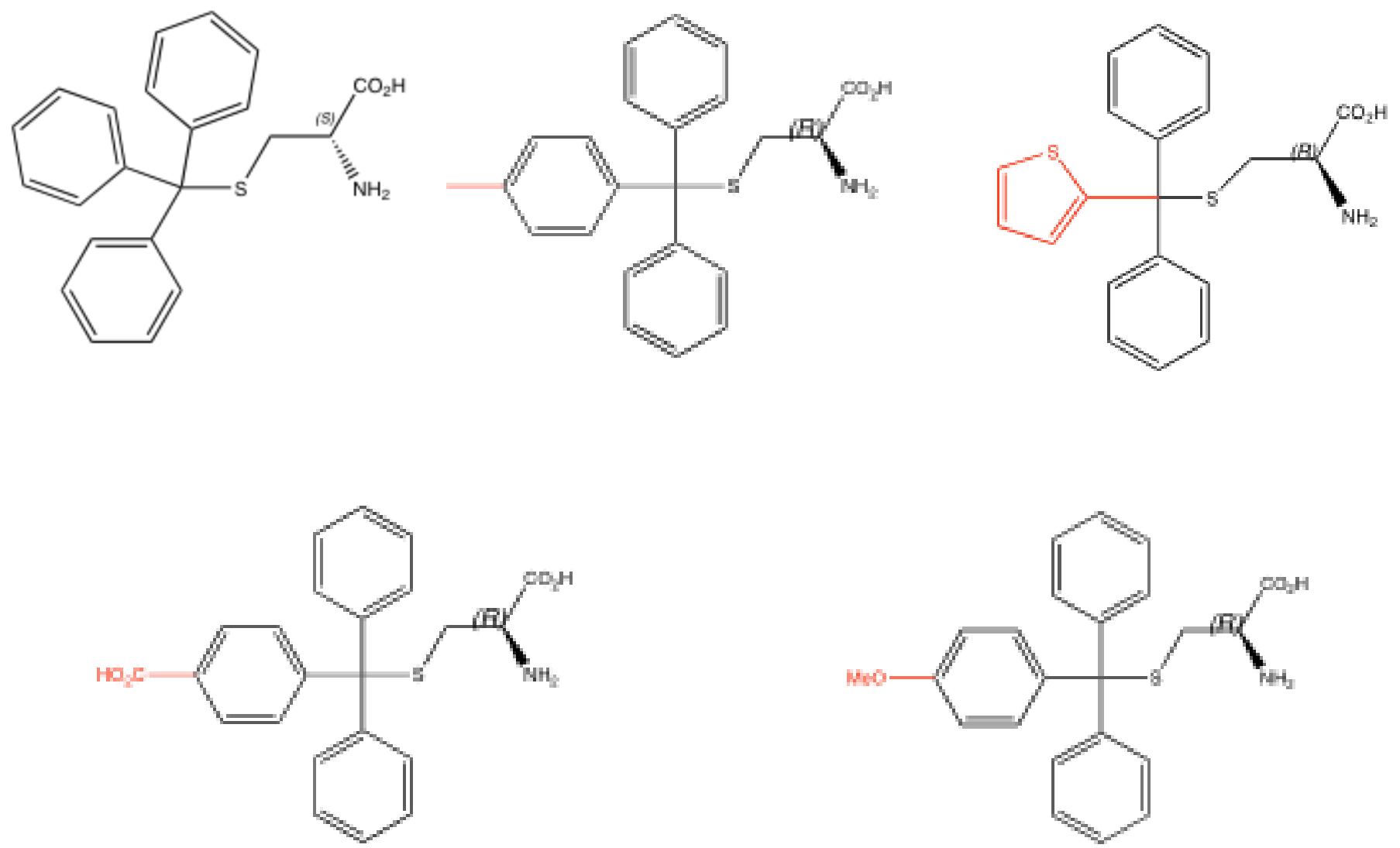


S-Trityl-L-Cysteine

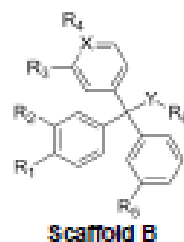
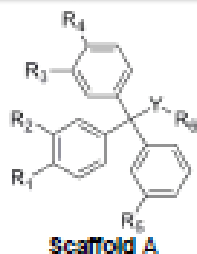


In figure are reported on the left STLCs derivative **51** (light brown) as proposed by Autodock and overlapped to **NSC 123526** (green) as docked into HCV-NS5B, and on the right derivative **51** as proposed in by DeBonis et al. (*J. Med. Chem.* **2008**, *51*, 1115–1125) in the Human Mitotic Kinesin Eg5 (HMKEg, Pdb entry code 2fme). To some extent compound **51** seems to bind either NS5B or HMKEg making similar interactions.

Focused Virtual Screening



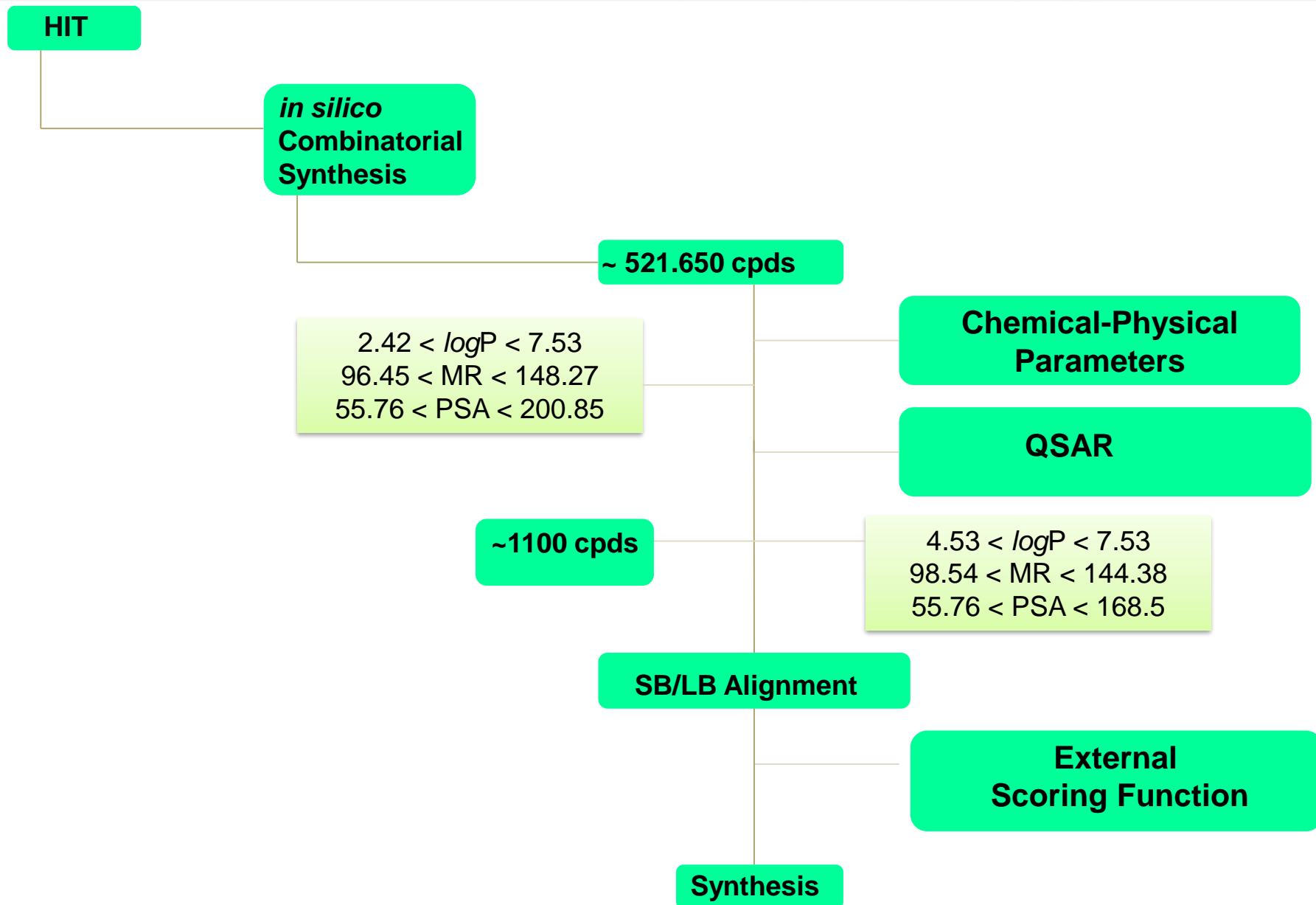
Focused Virtual Screening



Ref. *J.Med.Chem.* 2008, 51, 1115-1125

R ₁	R ₂	R ₃	R ₄	R ₆	X	Y	R ₆
Ref. Cl	H	H	H	H	C	S	
-CH ₃	-F		-OH protected	Cl	N		
-CH(CH ₃) ₂	-CH ₃						
-F							
-OH protected							
-SH protected							
-NH ₂ protected							
-OCH ₃							
-CF ₃							
-CN							

Focused Virtual Screening



ACKNOWLEDGMENTS

Prof. Rino Ragno
Prof. Antonello Mai
Prof. Neerja Kaushik-Basu
Dr. Sergio Valente

Adele Piroli
Alberto De Petris
Alexandros Patsilinakos
Anna Lucia Fallacara
Antonia Caroli
Antonio Coluccia
Fabio Onori
Federica De Mitri
Flavio Ballante
Girolamo Capezzer
Laura Silvestri

Luca Carioti
Marco Di Nocco
Mario Esposito
Paolo Mugione
Raffaele Maio
Riccardo De Santis
Roberta Fazi
Silvia Simeoni
Vanessa Torino
Yuri Zanni